Original Article
Investigating novel biomarkers in uterine corpus endometrial carcinoma: in silico analysis and clinical specimens validation via RT-qPCR and immunohistochemistry

Jie Li[1], Faiqah Ramzan[2], Guiping Zhong[1]

[1]Health Management Center, The Second Affiliated Hospital of Hainan Medical University, Haikou 570311, Hainan, China; [2]Gomal Center of Bio-Chemistry and Biotechnology (GCBB), Gomal University, Dera Ismail Khan 29050, Pakistan

Abstract: The rising incidence and mortality rate of Uterine Corpus Endometrial Carcinoma (UCEC) pose significant health concerns. CC and CXC chemokines have been linked to tumorigenesis and cancer progression. Recognizing the growing significance of CC and CXC chemokines' diagnostic and prognostic significance in diverse cancer types, our objective was to comprehensively analyze the diagnostic and prognostic values of hub genes from the CC and CXC chemokines in UCEC, utilizing both in silico and clinical samples and cell lines-based approaches. In silico analyses include STRING, Cytoscape, Cytohubba, The Cancer Genome Atlas (TCGA) datasets analysis via the UALCAN, GEPIA, OncoDB, and MuTarget, SurvivalGenie, MEXPRESS, cBioPoratal, TIMER, ENCORI, and DrugBank. Meanwhile, clinical samples and cell lines based analyses include Reverse transcription-quantitative polymerase chain reaction (RT-qPCR), targeted bisulfite sequencing (bisulfite-seq) analysis, and immunohistochemistry (IHC). Through present study, we identified CCL25 (CC motif chemokine ligand 25), CXCL10 (C-X-C motif chemokine ligand 10), CXCL12 (C-X-C motif chemokine ligand 12), and CXCL16 (C-X-C motif chemokine ligand 16) as crucial hub genes among the CC and CXC chemokines. Analyzing the expression data from TCGA, we observed a significant up-regulation of CCL25, CXCL10, and CXCL16 in UCEC samples compared to controls. In contrast, we noted a significant down-regulation of CXCL12 expression in UCEC samples. On clinical UCEC samples and cell lines analysis, the significant higher expression of CCL25, CXCL10, and CXCL16 and significant lower expression of CXCL12 were also denoted in UCEC samples than the controls via RT-qPCR and IHC analyses. Moreover, in silico analysis also confirmed the abnormal promoter methylation levels of the hub genes in TCGA UCEC samples, which was later validated by the clinical samples using targeted based bisulfite-seq analysis. In addition, various additional aspects of the CCL25, CXCL10, CXCL12, and CXCL16 have also been uncovered in UCEC during the present study. Our findings offer novel insights that contribute to the clinical utility of CCL25, CXCL10, CXCL12, and CXCL16 chemokines as potential diagnostic and prognostic biomarkers in UCEC.

Keywords: UCEC, CC and CXC chemokines, biomarkers

Introduction

Uterine Corpus Endometrial Carcinoma (UCEC) is one of the most common gynecologic cancers affecting women today [1]. It refers to cancer that develops in the lining of the uterus or endometrium [2, 3]. According to the National Cancer Institute, there were approximately 61,880 new cases of endometrial cancer in the United States in 2021, and the mortality rate is reported to be around 12,160 [4].

Despite the advancements in the diagnosis and management of UCEC, it remains a significant health issue, primarily due to the lack of reliable diagnostic and prognostic biomarkers [5, 6]. The identification of novel biomarkers could help in early detection, improved risk assessment, and personalized treatment options for women with UCEC [7]. The current diagnostic methods for UCEC include endometrial biopsy, dilation and curettage, and imaging tests [8]. However, these methods are prone to diagnos-

tic error. Hence, there is a need for specific biomarkers that could detect UCEC more sensitively. Additionally, prognostic biomarkers are needed to identify patients with more aggressive disease who may benefit from more aggressive treatment.

The intricate interplay between the immune system and cancer progression has emerged as a captivating area of exploration, garnering considerable attention and extensive research efforts throughout the years [9]. Chemokines, classified as a group of cytokines, are produced by various cell types such as tumor cells, leukocytes, immune cells, and others. These molecules have been recognized for their crucial role in modulating inflammation and immune responses [10]. Chemokines can be categorized into four primary subgroups (CXC, CC, C, and CX3C) based on the number and position of the first two conserved cysteine residues located at the N terminus [11]. Chemokines are also classified into distinct subsets based on their functions and expression patterns, namely homeostatic and inflammatory chemokines [12]. Inflammatory chemokines are typically induced during instances of inflammation and are expressed by various cell types, including leukocytes [12]. These chemokines play a crucial role in facilitating the recruitment of inflammatory leukocytes to the site of tissue damage or inflammation [13, 14]. In contrast, homeostatic chemokines exhibit continuous expression in specific tissues even in the absence of obvious activating stimuli [12]. These chemokines play a vital role in regulating cellular trafficking and maintaining the proper functioning of immune surveillance systems [13-15]. CC and CXC chemokines play critical roles in tumor angiogenesis, growth, invasion, and metastasis, showcasing their significance in these processes [11, 16].

Recent studies have delved into the examination of expression patterns, diagnostic, and prognostic implications of CXC and CC chemokine member in diverse human cancers, such as colon cancer, gastric cancer, hepatocellular carcinoma, and non-small-cell lung cancer [17-22]. Therefore, the objective of this study was to perform a comprehensive analysis, combining in silico and in vitro approaches, to uncover the diagnostic and prognostic significance of the complete CXC and CC chemokine families in UCEC.

Methodology

UCEC and normal control tissue samples collection

Following the approval of the ethics committee at the Gomal University, Dera Ismail Khan, Pakistan, we conducted a prospective collection of 25 pairs of UCEC tissue samples diagnosed with endometrioid carcinoma (EC) and corresponding normal tissues from patients who visited the Institute of Nuclear Medicine, Oncology and Radiotherapy Hospital and Ayub Medical Complex between August 2022 and May 2023. Prior to their participation, all individuals provided informed consent by signing consent forms. All patients included in the study were diagnosed with UCEC and had not undergone adjuvant or neoadjuvant therapy prior to surgery.

Construction of the CC and CXC families member PPI and the selection of hub genes

Utilizing the STRNG (https://string-db.org/) database [23], we generated protein-protein interaction (PPI) networks for Member of the CC and CXC chemokine Families. Subsequently, the Cytohubba function [24] within the Cytoscape tool was employed to screen the critical module and identify the hub genes. To ensure a comprehensive selection of hub genes, we applied four distinct scoring algorithms: the maximum neighborhood component (MNC), the density of the maximum neighborhood component (DMNC), the maximal clique centrality (MCC), and the Degree of the Cytohubba [25]. Each algorithm brought a unique perspective to the network analysis. Through a consensus approach, the shared top four genes that emerged from these four algorithms were meticulously chosen as the hub genes. This methodological blend of multiple scoring algorithms minimized bias and increased the robustness of our findings.

UALCAN database

The UALCAN database (http://ualcan.path.uab.edu/) offers comprehensive analysis of cancer-related omics data sourced from The Cancer Genome Atlas (TCGA) and MET500 databases [26]. The mRNA expression levels of the identified hub genes in both UCEC and normal tissues were examined utilizing the "TCGA gene

analysis" module of the UALCAN database with default settings. For statistical purpose, a student t-test was employed in UALCAN.

GEPIA, OncoDB, and MuTarget databases

For additional validation of the expression of hub genes in UCEC tissues and normal controls, we utilized multiple online databases including GEPIA (http://gepia.cancer-pku.cn/) [27], OncoDB (https://oncodb.org/) [28], and MuTarget (https://www.mutarget.com/) [29] with defaults settings. These databases are renowned platforms for cancer microarray-based expression analysis, offering comprehensive results in the form of box plots. For statistical purpose, a student t-test was used by these databases.

Survival analysis

SurvivalGenie (https://bbisr.shinyapps.winship. emory.edu/SurvivalGenie/) is an innovative tool used for survival analysis in biomedical research [30, 31]. It offers a user-friendly interface and robust statistical algorithms to analyze survival data, such as Kaplan-Meier curves, Cox proportional hazards models, and log-rank tests. With its intuitive features, SurvivalGenie empowers researchers to gain valuable insights into the survival outcomes of patients in various studies, contributing to advancements in clinical and translational research. In this study, survival analysis of the hub genes was performed using log-rank test with default settings via SurvivalGenie.

MEXPRESS analysis

To assess the DNA promoter methylation levels of the identified hub genes in UCEC patients, we utilized the MEXPRESS (https://mexpress. be) [32] database with defaults settings. MEXPRESS is a powerful tool that visualizes the correlations between patient clinical information and promoter methylation levels across TCGA datasets. For statistical purpose, a student t-test was employed in MEXPRESS.

cBioPortal analysis

The cBioPortal (https://www.cbioportal.org/), an online open-access platform [33, 34], was utilized to perform multidimensional cancer genomic analysis on TCGA cancer datasets.

This database enables the querying of gene(s) of interest and facilitates the exploration of relevant alterations across over 5,000 cancer samples from 20 different cancer studies. The cBioPortal was conducted in this study with default settings for analyzing genetic mutations and co-express genes in UCEC patients.

Functional enrichment analysis

In this study, the functional enrichment analysis of the hub genes was performed using the GSEA program with defaults parameters. This analysis included Gene Ontology (GO) and Kyoto Encyclopedia of Genes and Genomes (KEGG) analyses. By considering the biological characteristics of the studied protein or gene list, the GSEA program identified relevant GO terms and KEGG pathways [35]. For statistical purpose, a student t-test was employed in GSEA.

TIMER database

To evaluate the infiltration of immune cells within tumors, the web-based TIMER database (http://timer.cistrome.org/) [36] was employed with default settings. This database employs various algorithms to estimate the abundance of immune cells across different types of cancer. In this research, the levels of immune cell infiltration in UCEC were plotted against the expression levels of the identified hub genes to find Pearson correlation. For statistical purpose, a student t-test was employed in TIMER.

miRNA network of the hub genes'

The ENCORI database (https://rnasysu.com/encori/), known for its exploration of MicroRNA (miRNA)-Noncoding RNA (ncRNA) and Messenger RNA (mRNA)-miRNA interactions using CLIP-seq and degradome-seq interactome data [37] was utilized in this study. Specifically, the ENCORI database was employed with default parameters to construct the miRNA network associated with the identified hub genes.

Hub genes' drug prediction analysis

In the present study, we performed the DrugBank (https://go.drugbank.com/) [38] research to find the drugs related to the hub genes because we believe that the identified

hub genes can be interesting therapeutic targets.

Experimental validation of the hub gene expression and methylation status on clinical samples and cell lines

Cell line culturing: Two endometrial adenocarcinoma cell lines, including AN3CA (HTB-111) and HEC-1-A (HTB-112), while one normal endometrial cell line HES, were purchased from American Type Culture Collection (Manassas, VA, USA). All cell lines were cultured in Dulbecco's modified Eagle's medium (DMEM; Biochrom, Ltd., Berlin, Germany), supplemented with 10% fetal calf serum (FCS; Biochrom, Ltd.) and 1% penicillin/streptomycin (P/S) (Biochrom, Ltd.).

RNA and DNA extraction: The extraction of total RNA from both clinical tissue samples, cell lines, and normal control samples was carried out using the isopycnic centrifugation method as previously described [36]. DNA extraction was performed using the organic method [37]. The quality of the extracted RNA and DNA was assessed using a 2100 Bioanalyzer (Agilent Technologies, Germany).

Reverse transcription-quantitative polymerase chain reaction (RT-qPCR) validation analysis of hub genes

The specific protocols are as follows: First, the PrimeScript™ RT reagent kit (Takara, Japan) was used for reverse transcription of the extracted RNA from tissue samples, AN3CA (HTB-111) and HEC-1-A (HTB-112), and HES cell lines into complementary DNA. Then, the RT-qPCR was carried out on an ABI ViiA 7 Real Time PCR System (Thermo Fisher, USA) with a SuperReal SYBR Green Premix Plus (Tiangen Biotech, China) as a fluorescent dye. GAPDH was chosen as the internal reference in the present study. All the experiments were in triplicate independently. All the primers of each hub gene are shown as following. The 2-ΔΔCt method was employed to evaluate the relative expression of each hub gene [39]. For statistical purpose, a student t-test was employed on RT-qPCR data.

GAPDHF 5'-ACCCACTCCTCCACCTTTGAC-3', GAPDHR 5'-CTGTTGCTGTAGCCAAATTCG-3' [40]. CCL25F 5'-AAGGCCCAGAGTTACTATCGC-3', CC-

L25R 5'-TCTTCATCCCAGCCTGAACC-3' [41]. CXCL10F 5'-GCTCAGGCTCGTCAGTTCTAAGT-3', CXCL10R 5'-GGAAGATGGTGGTTAAGTTCGTC-3' [42]. CXCL12F 5'-TCAGCCTGAGCTACAGATGC-3', CXCL12R 5'-CTTTAGCTTCGGGTCAATGC-3' [43]. CXCL16F 5'-CTGACTCAGCCAGGCAATGG-3', CXCL16R 5'-TGAGTGGACTGCAAGGTGGA-3' [44].

RT-qPCR analysis of hsa-miR-744-5p expression

To analyze hsa-miR-744-5p expression in clinical UCEC samples, we conducted RT-qPCR using the PrimeScript® miRNA RT-PCR kit (Takara) following the guidelines provided by the manufacturer. All the experiments were in triplicate independently. For normalization of miRNA expression, U6 snRNA was utilized in this analysis. The relative expression levels were determined using the 2-ΔΔCt method [39] and student t-test was used to evaluate differences in the expression levels between UCEC and normal control group. Following primers were used for the expression analysis of hsa-miR-744-5p and U6.

U6-F 5'-CTCGCTTCGGCAGCACA-3', U6-R 5'-AACGCTTCACGAATTTGCGT-3'; Hsa-miR-744-5p-F 5'-AATGCGGGGCTAGGGCTA-3', Hsa-miR-744-5p-R 5'-GTGCAGGGTCCGAGGT-3' [45].

Library preparation for targeted bisulfite sequencing analysis

In brief, total DNA (1 µg) was fragmented into approximately 200-300 bp fragments using a Covarias sonication system (Covarias, Woburn, MA, USA). Following purification, the DNA fragments underwent repair and phosphorylation of blunt ends using a mixture of T4 DNA polymerase, Klenow Fragment, and T4 polynucleotide kinase. The repaired fragments were then 3' adenylated using Klenow Fragment (3'-5' exo-) and ligated with adapters containing 5'-methylcytosine instead of 5'-cytosine and index sequences using T4 DNA Ligase. The constructed libraries were quantified using a Qubit fluorometer with the Quant-iT dsDNA HS Assay Kit (Invitrogen, Carlsbad, CA, USA) and sent to Beijing Genomic Institute (BGI), China for targeted bisulfite sequencing. Following sequencing, the methylation data was normalized into beta values.
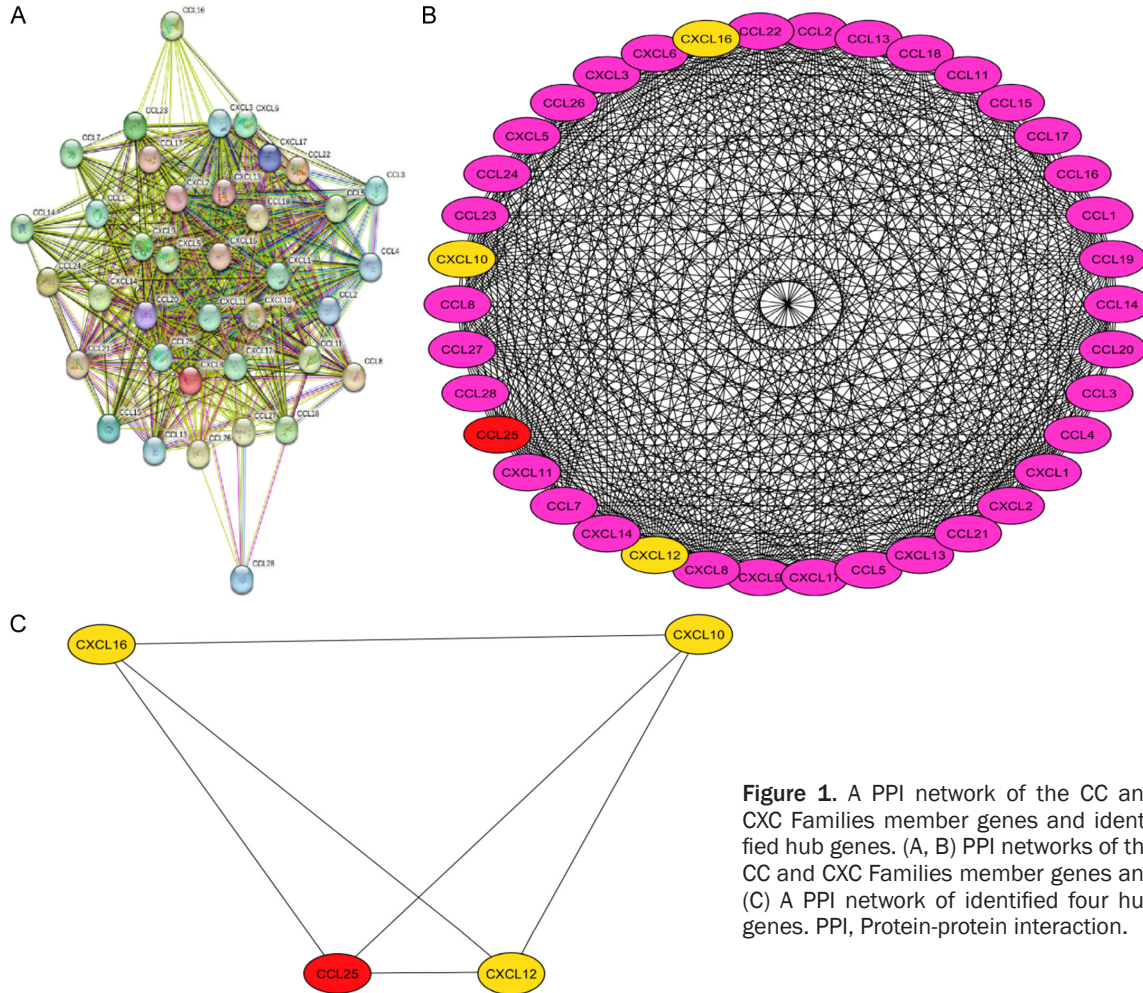
Figure 1. A PPI network of the CC and CXC Families member genes and identified hub genes. (A, B) PPI networks of the CC and CXC Families member genes and (C) A PPI network of identified four hub genes. PPI, Protein-protein interaction.

Immunohistochemical validation of the hub genes in clinical samples

For this study, IHC staining was performed on both UCEC and normal samples. The cancer and normal tissues were fixed in formalin and embedded in paraffin wax. Subsequently, sections of the tissues were obtained. The tissue sections underwent a sequential treatment with alcohol, starting with xylene, followed by a series of decreasing alcohol concentrations (100%, 95%, 90%, 80%, and 70%). Tissue antigen retrieval was achieved through boiling with sodium citrate buffer, while endogenous peroxidase inhibitors were added to inhibit peroxidase activity. To prevent non-specific binding, the tissue sections were blocked in 5% goat serum for 1 hour. Following that, separate drops of anti-CCL25, CXCL10, CXCL12, and CXCL16 antibodies (dilution ratio: 1:300; 25285-1-AP, CXCL10/IP10, CXCL12/SDF-1,

and MAB503-SP) were applied onto the sections and incubated overnight at 4°C. Subsequently, secondary antibody (anti-rabbit) was added and incubated. Afterward, diaminobenzidine was introduced for color development, followed by hematoxylin re-staining. Finally, the staining results were assessed by blocking and photographing the sections.

Results

Construction of the CC and CXC families' member PPI and the selection of hub genes

To establish a threshold for interaction scores, a minimum value of > 0.4 was selected. Subsequently, proteins belonging to the CC and CXC chemokine families were analyzed using STRING to construct the PPI. The resulting PPI network, as visually depicted in **Figure 1A** and **1B**, revealed a remarkable interconnected-

ness, featuring a total of 267 edges interlinking 38 distinct nodes. To identify the hub genes within this network, we employed a combination of scoring algorithms, including MNC, DMNC, MCC, and Degree, through the Cyto-Hubba tool. The top four shared DEGs by these 4 algorithms were regarded, including CCL25 (CC motif chemokine ligand 25), CXCL10 (C-X-C motif chemokine ligand 10), CXCL12 (C-X-C motif chemokine ligand 12), and CXCL16 (C-X-C motif chemokine ligand 16) were regarded as the hub genes (**Figure 1C**).

Hub genes expression profiling via UALCAN

Having identified CCL25, CXCL10, CXCL12, and CXCL16 as hub genes, we proceeded to analyze the expression levels of these genes in TCGA UCEC samples and normal controls using the UALCAN database. This analysis provided insights into the differential expression patterns of these hub genes in UCEC compared to normal tissues. The analysis revealed that the expression of CCL25, CXCL10, and CXCL16 was significantly up-regulated in UCEC samples compared to controls (**Figure 2A**, **2B**). Conversely, the hub gene CXCL12 showed a notable down-regulation in UCEC samples (**Figure 2A**, **2B**). These careful observations highlight a significant (P < 0.05) dysregulation of these hub genes, suggesting that they might play important roles in the complex development of UCEC.

Additionally, when considering different clinical variables such as cancer stage, race, age, and menopause status, it was observed that the expression levels of CCL25, CXCL10, and CXCL16 were consistently higher (P < 0.05), while the expression of CXCL12 was consistently lower (P < 0.05) in UCEC patients relative to the control samples (**Figure 3**). These results not only show dysregulation of hub genes, but also suggest that these genes could be useful markers for UCEC patients of different clinical variables.

Verification of the hub genes expression

To further validate the expression of the hub genes, we conducted expression validation analysis using additional TCGA datasets through the GEPIA, OncoDB, and MuTarget databases. The results, depicted in **Figure 4A-D**, demonstrated that the mRNA expression

levels of CCL25, CXCL10, and CXCL16 were significantly (P < 0.05) elevated in UCEC samples compared to normal individuals. Conversely, the mRNA expression of CXCL12 was notably (P < 0.05) lower in UCEC samples. These remarkable consistencies, observed across multiple independent TCGA datasets, serve as a compelling validation of our earlier findings, further provided evidences of hub gene dysregulation as a hallmark of UCEC pathogenesis.

Survival analysis of CCL25, CXCL10, CXCL12, and CXCL16

In this study, we utilized the SurvivalGenie tool to conduct survival analysis on CCL25, CXCL10, CXCL12, and CXCL16 genes in UCEC patients. The analysis revealed a significant (P < 0.05) association between the dysregulation of these genes and poor overall survival (OS) in UCEC patients (**Figure 5**). This finding suggests that alterations in the expression levels of CCL25, CXCL10, CXCL12, and CXCL16 may serve as prognostic indicators for UCEC patients, highlighting the potential of these genes as important prognostic biomarkers in assessing OS and guiding clinical decision-making in UCEC management.

Promoter methylation analysis of CCL25, CXCL10, CXCL12, and CXCL16

To assess the potential influence of promoter methylation on the dysregulation of CCL25, CXCL10, CXCL12, and CXCL16 hub genes' expression in UCEC, we examined their mRNA expressions in relation to promoter methylation using MEXPRESS. This analysis aimed to determine whether the expression levels of CCL25, CXCL10, CXCL12, and CXCL16 were regulated by promoter methylation in UCEC or not. Remarkably, our analysis revealed intriguing findings regarding the promoter methylation levels of the hub genes. Specifically, we observed a significant (P < 0.05) hypomethylation in the promoters of CCL25, CXCL10, and CXCL16 genes, whereas the promoter of CXCL12 exhibited hypermethylation in UCEC specimens compared to controls (**Figure 6**). These results suggest that the higher expression of CCL25, CXCL10, and CXCL16, as well as the lower expression of CXCL12, can be attributed to the abnormal promoter methylation levels in UCEC. Thus, it can be concluded that the dysregulation of these hub genes in UCEC is
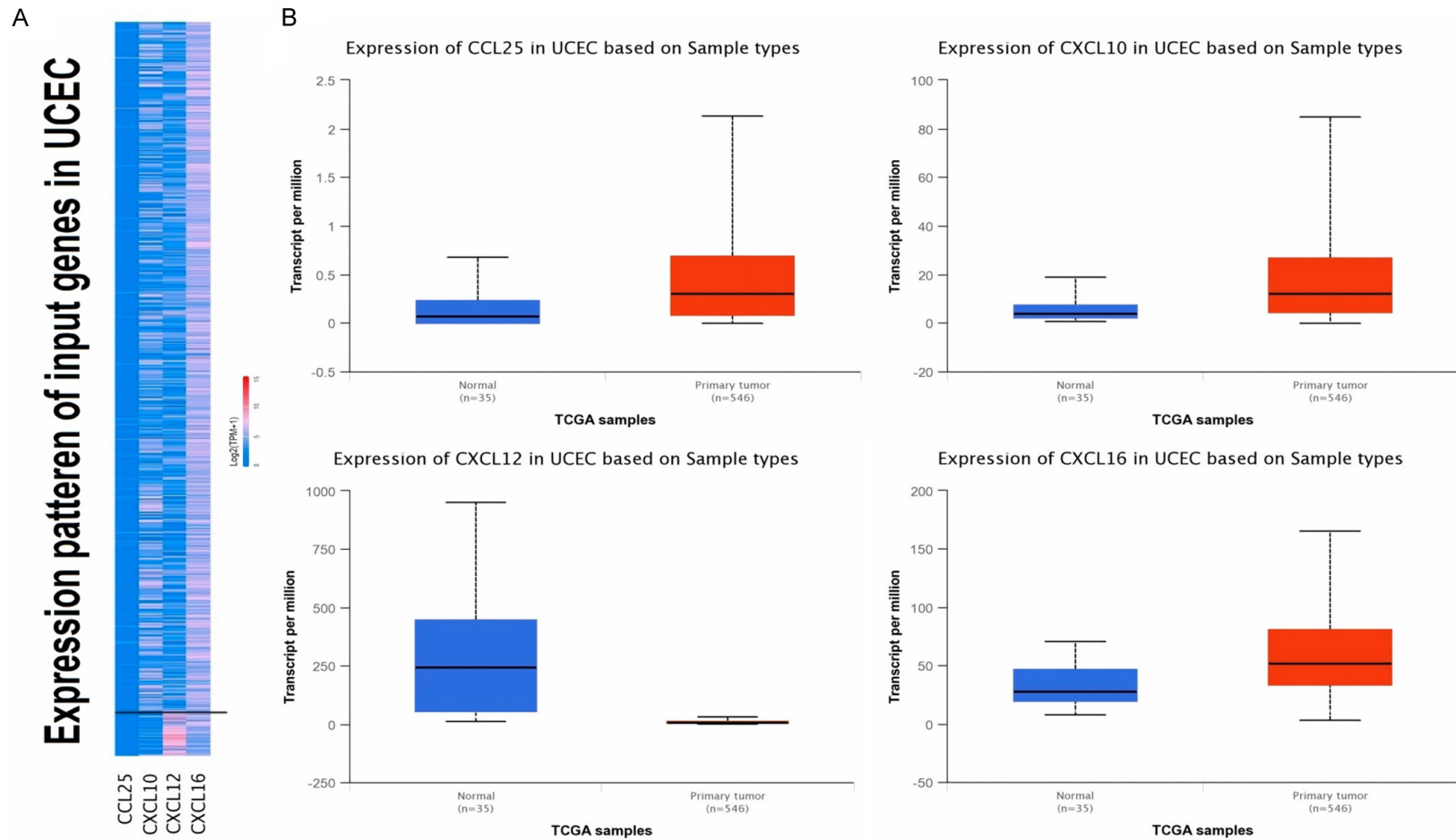
Figure 2. Expression profiling of the CCL25, CXCL10, CXCL12, and CXCL16 in UCEC samples paired with controls via UALCAN. (A) A heatmap of CCL25, CXCL10, CXCL12, and CXCL16 hub genes in UCEC sample group and normal control group and (B) Box plot presentation of CCL25, CXCL10, CXCL12, and CXCL16 hub genes expression in UCEC sample group and normal control group. A *p*-value less than 0.05 was considered as significant. UCEC, Uterine Corpus Endometrial Carcinoma.
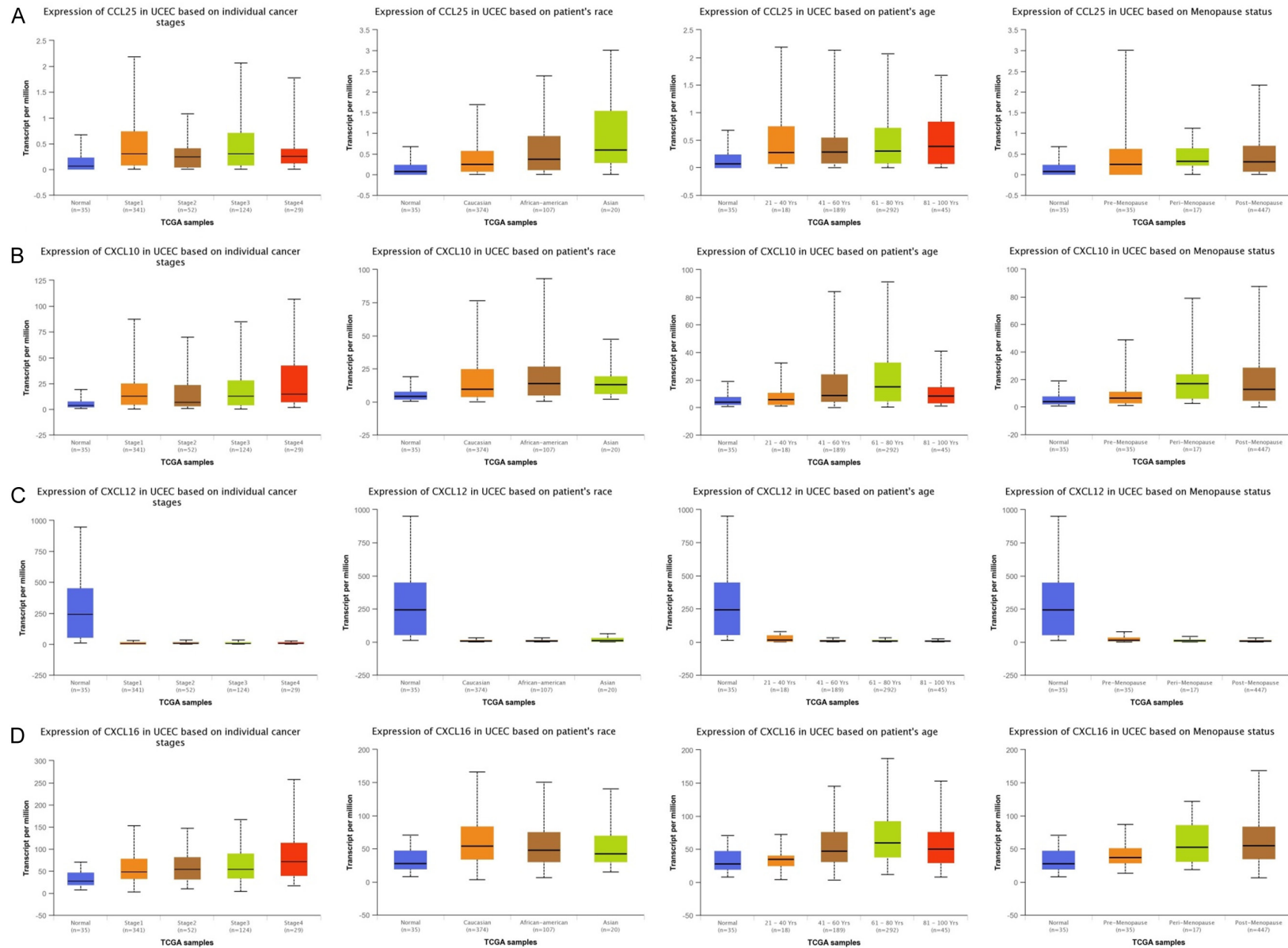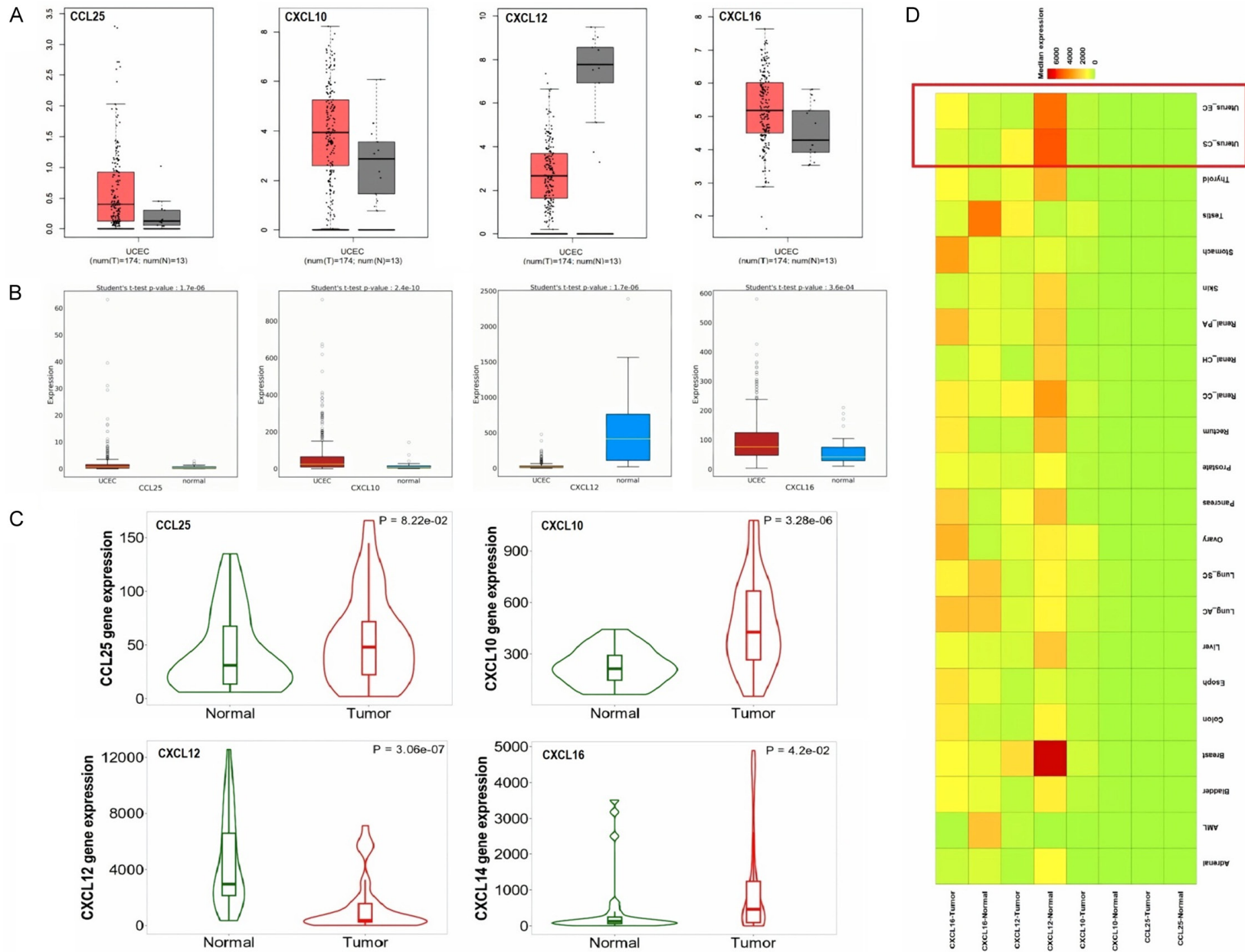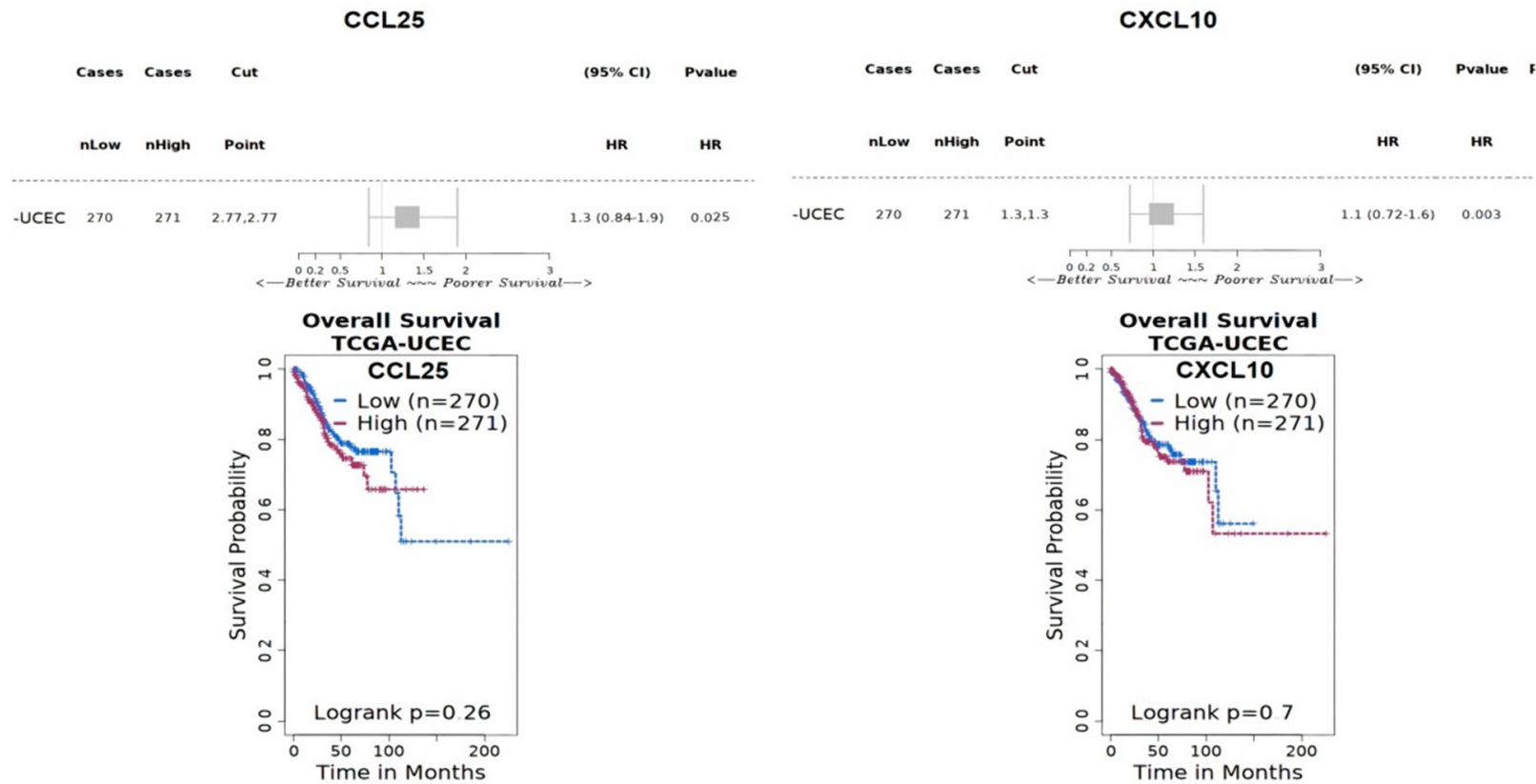
Figure 3. Expression profiling of CCL25, CXCL10, CXCL12, and CXCL16 in UCEC samples of different clinical variables relative to controls via UALCAN. (A) Expression profiling of CCL25 in UCEC samples of different clinical variables, (B) Expression profiling of CXCL10 in UCEC samples of different clinical variables, (C) Expression profiling of CXCL12 in UCEC samples of different clinical variables, and (D) Expression profiling of CXCL16 in UCEC samples of different clinical variables. A *p*-value less than 0.05 was considered as significant. UCEC, Uterine Corpus Endometrial Carcinoma.

Figure 4. Expression validation of CCL25, CXCL10, CXCL12, and CXCL16 using additional TCGA datasets. (A) Expression validation of CCL25, CXCL10, CXCL12, and CXCL16 in UCEC and normal samples via GEPIA database, (B) Expression validation of CCL25, CXCL10, CXCL12, and CXCL16 in UCEC and normal samples via OncoDB database, (C) Expression validation of CCL25, CXCL10, CXCL12, and CXCL16 in UCEC and normal samples via MuTarget database, and (D) Expression heatmap of CCL25, CXCL10, CXCL12, and CXCL16 in UCEC and normal samples via MuTarget database. A *p*-value less than 0.05 was considered as significant. UCEC, Uterine Corpus Endometrial Carcinoma.

Figure 5. Survival analysis of CCL25, CXCL10, CXCL12, and CXCL16 in UCEC patients using SurvivalGenie database. A *p*-value less than 0.05 was considered as significant. UCEC, Uterine Corpus Endometrial Carcinoma.
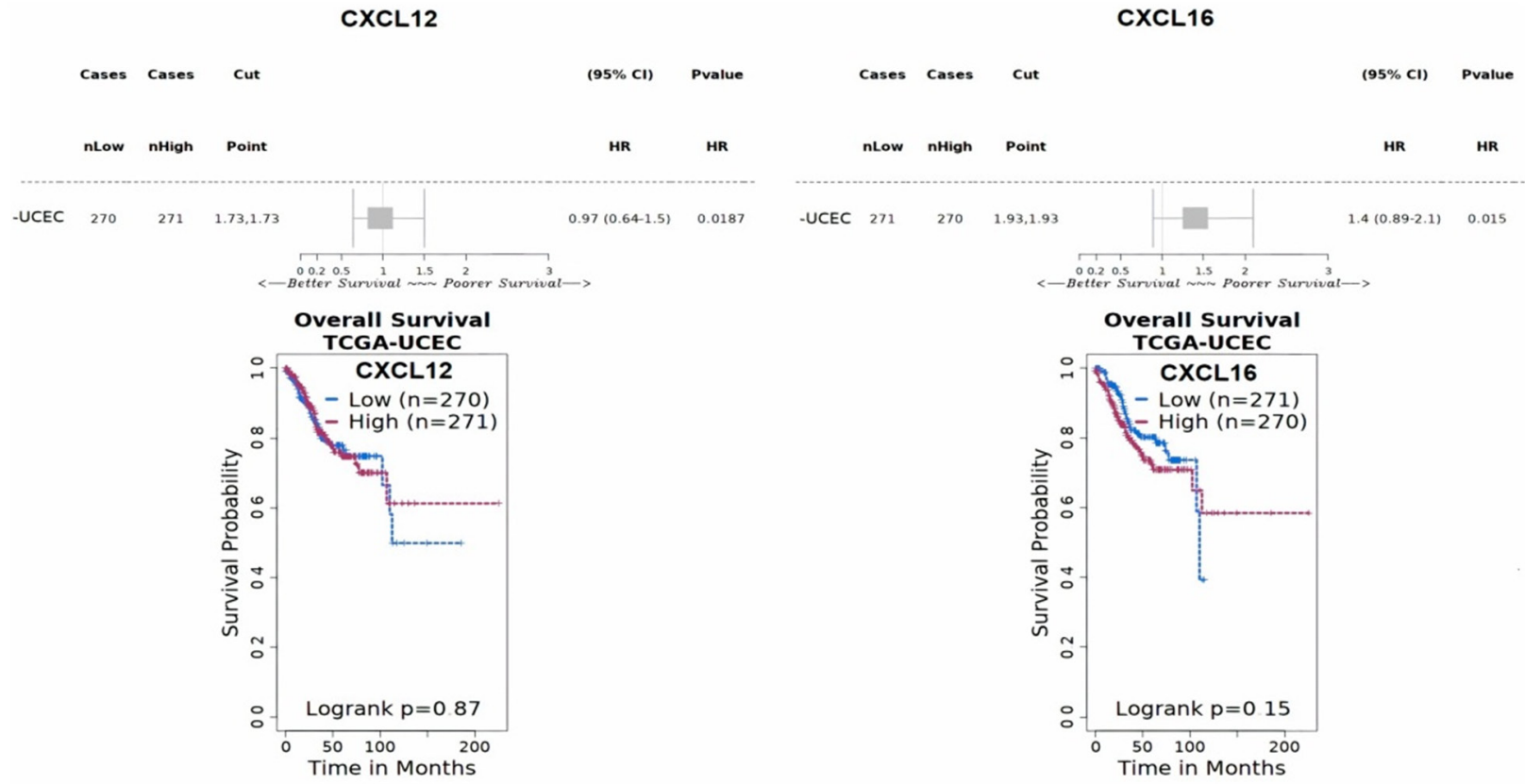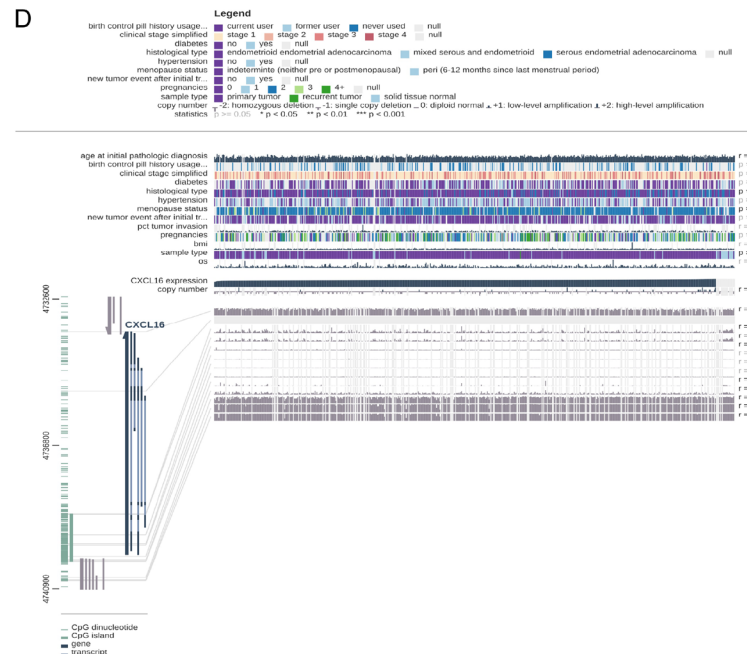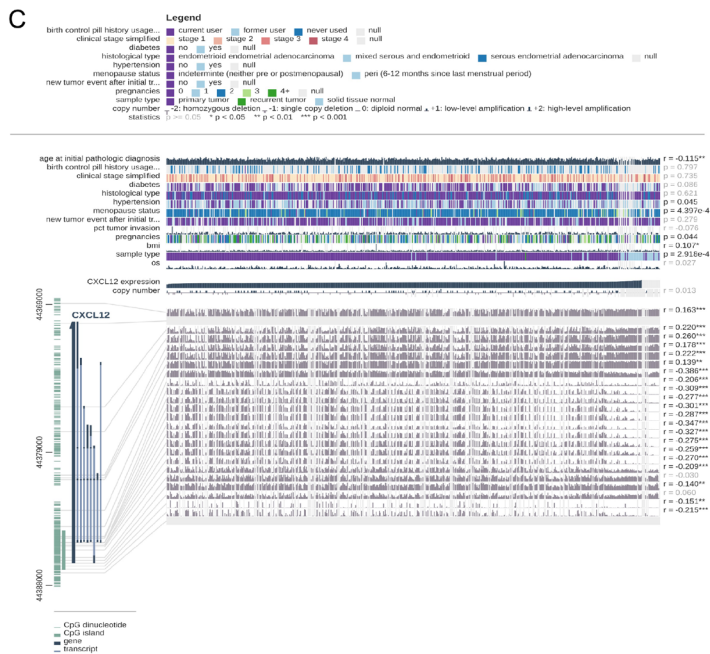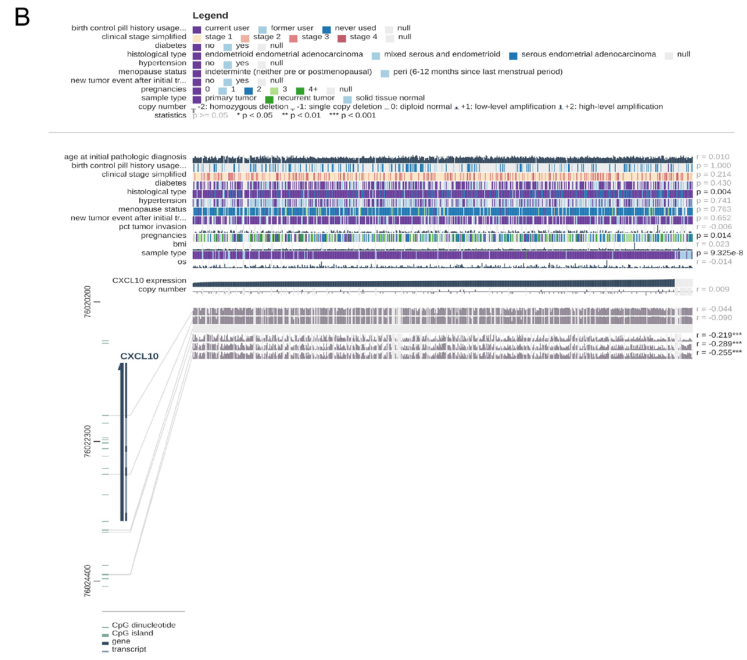
UCEC-associated novel biomarkers

Figure 6. Methylation status exploration of CCL25, CXCL10, CXCL12, and CXCL16 via MEXPRESS in UCEC and normal samples. (A) CCL25, (B) CXCL10, (C) CXCL12, and (D) CXCL16. A *p*-value less than 0.05 was considered as significant. UCEC, Uterine Corpus Endometrial Carcinoma.

associated with their respective promoter methylation patterns.

Mutational and co-express gene analyses of CCL25, CXCL10, CXCL12, and CXCL16

Using the cBioPortal database, we conducted mutational and co-express gene analyses for CCL25, CXCL10, CXCL12, and CXCL16 in UCEC patients. Among the analyzed UCEC samples, the CCL25 gene exhibited the highest frequency of genetic alterations, observed in 2.1% of the total samples (**Figure 7A**). In the analyzed UCEC samples, the alteration rates for CXCL10, CXCL12, and CXCL16 were found to be 0.8%, 1.7%, and 1.7% respectively. Additionally, it was noted that deep amplification was the predominant factor contributing to the changes observed in the analyzed hub genes (**Figure 7A**).

Additionally, by performing co-expressed gene analysis, we calculated correlation coefficients and identified that along with CCL25, MYBBP-1A was a significant co-expressed gene in UCEC samples (**Figure 7B**), while CARD11, TES, and LRRC37B were the highly co-expressed genes in UCEC samples with CXCL10, CXCL12, and CXCL16, respectively (**Figure 7B**). These close connections between genes show that they might dysregulate together in UCEC patients. This important information gives us a hint about how these genes team up in the development and progression of UCEC.

Functional enrichment analysis

GO and KEGG enrichment analyses of hub genes (CCL25, CXCL10, CXCL12, and CXCL16) were done with the help of DAVID tool. In this study, "Nucleocytoplasmic transport complex, CBM complex, and External side of plasma membrane" were the major cellular components (CC) of the hub genes (**Figure 8A**). "CCR10 chemokine receptor binding, CXCR3 chemokine receptor binding, CXCR chemokine receptor binding, and Guanylate kinase activity etc.", molecular functions (MFs) were mainly associated with hub genes (**Figure 8B**), while "Neg. reg. of leukocyte tethering and rolling, Neg. reg. of leukocyte adhesion to vascular endothelial cell, and Neg. reg. of extracellular

extravasation etc." were the primary biological process (BP) of the hub genes (**Figure 8C**). Moreover, KEGG pathways for the identified hub genes are highlighted in **Figure 8D**, and "Intestinal immune network for IgA production, viral protein interaction with cytokine and cytokine receptor, Chemokine signaling pathways etc." were found to be involved in the pathogenesis of UCEC.

Immune cells analysis of the CCL25, CXCL10, CXCL12, and CXCL16

Subsequently, we utilized the "TIMER" tool to explore the associations between immune cell infiltration (CD8+ T cells, CD4+ T cells, and macrophages) and the expression of hub genes (CCL25, CXCL10, CXCL12, and CXCL16) in UCEC samples. We observed a significant (P < 0.05) positive correlation between the expression of CCL25, CXCL10, CXCL12, and CXCL16 hub genes and the abundance of CD8+ T immune cells in UCEC samples. Conversely, there was a negative correlation between the expression of these hub genes and the abundance of CD4+ T and macrophage immune cells in UCEC samples (**Figure 9**). This negative correlation implies that the expression of CCL25, CXCL10, CXCL12, and CXCL16 might be associated with a reduction in the infiltration of CD4+ T immune cells and macrophages. This phenomenon might be indicative of a mechanism through which the tumor microenvironment could potentially evade immune responses by modulating the expression of these hub genes.

miRNA-mRNA interaction network and analysis of hsa-mir-744-5p expression via RT-qPCR

Using ENCORI and Cytoscape, we created miR-NA-mRNA co-regulatory networks for CCL25, CXCL10, CXCL12, and CXCL16. In these networks, we identified a total of 85 miRNAs and 4 mRNAs (**Figure 10**). Notably, among these networks, we discovered a single miRNA (hsa-mir-744-5p) that targets all the hub genes simultaneously. This finding leads us to speculate that the hsa-mir-744-5p and the hub genes (CCL25, CXCL10, CXCL12, and CXCL16) may collectively play a role as potential inducers of UCEC.
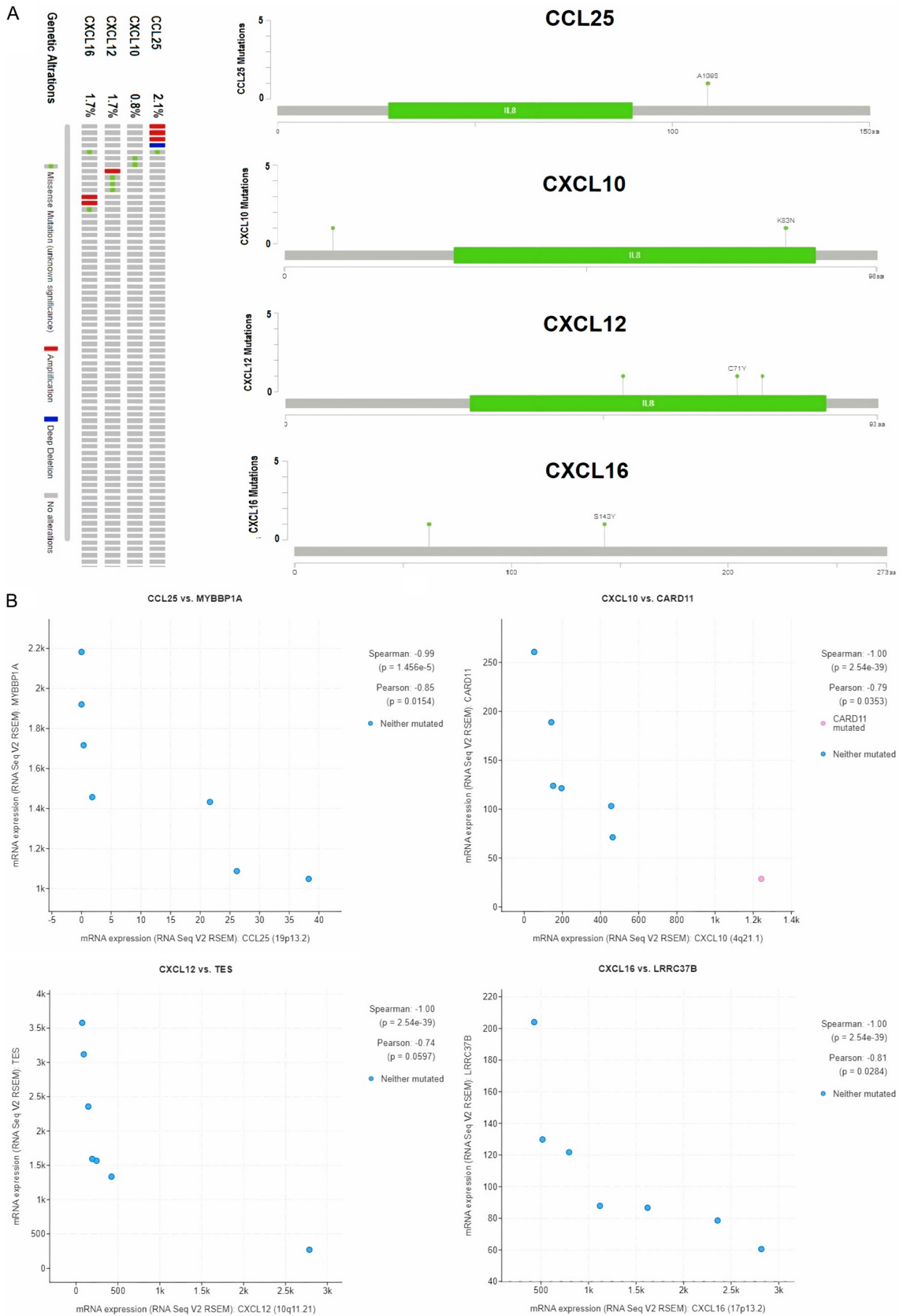
Figure 7. Exploration of genetic alteration frequencies and co-express genes with hub gens in UCEC samples via cBioPortal. (A) Frequencies, and location of the genetic alterations in CCL25, CXCL10, CXCL12, and CXCL16, and (B) Co-express genes with hub genes in UCEC groups. UCEC, Uterine Corpus Endometrial Carcinoma.
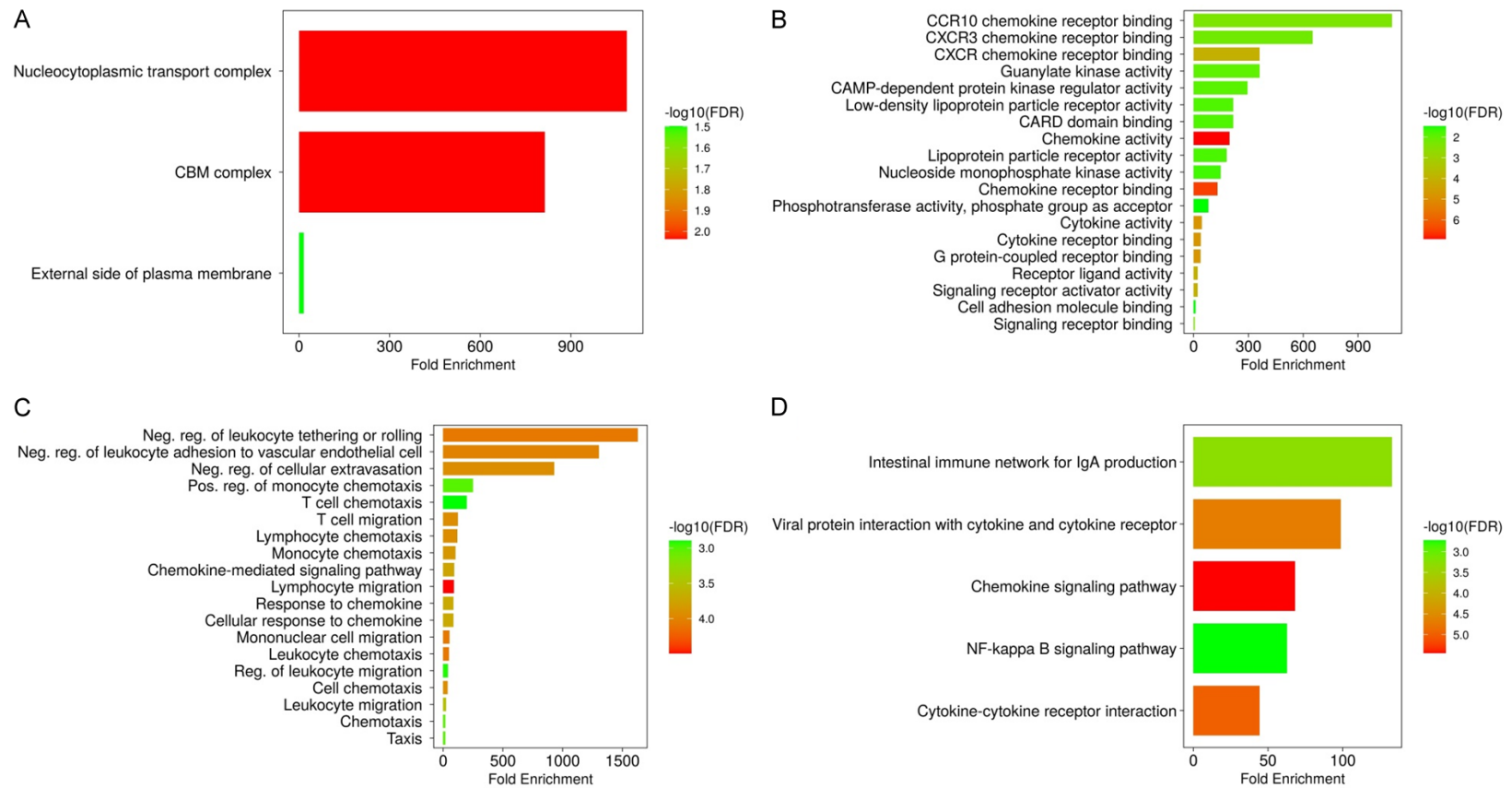
Figure 8. Gene enrichment analysis of CCL25, CXCL10, CXCL12, and CXCL16. (A) CCL25, CXCL10, CXCL12, and CXCL16 associated CC terms, (B) CCL25, CXCL10, CXCL12, and CXCL16 associated MF terms, (C) CCL25, CXCL10, CXCL12, and CXCL16 associated BP terms, and (D) CCL25, CXCL10, CXCL12, and CXCL16 associated KEGG terms. A *p*-value less than 0.05 was considered as significant. CC, Cellular components; MF, Molecular functions; BP, Biological process; KEGG, Encyclopedia of Genes and Genomes.
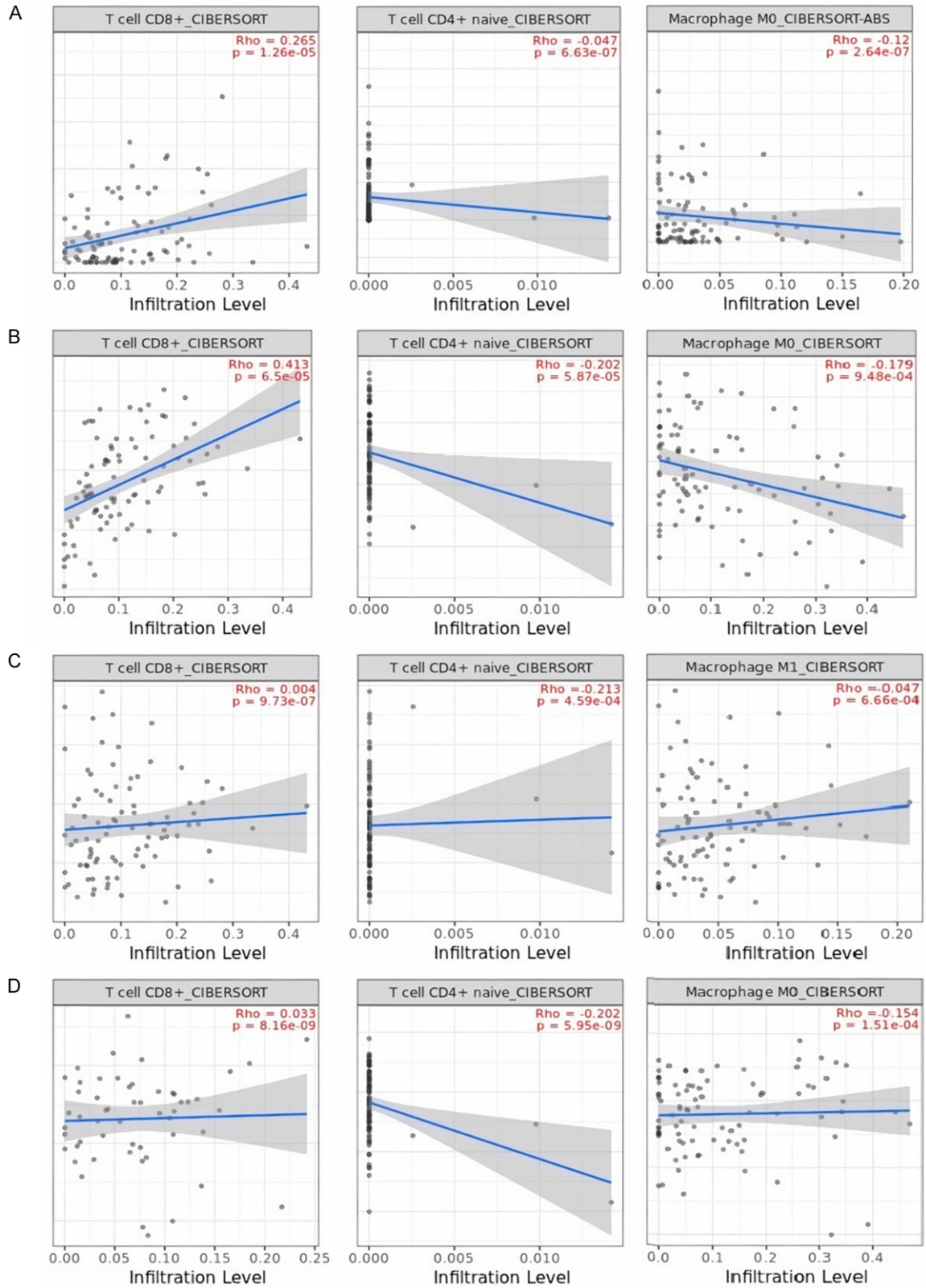
Figure 9. Correlation analysis of CCL25, CXCL10, CXCL12, and CXCL16 hub genes expression with different immune cells (CD8+ T, CD4+ T, and macrophages) infiltration level. (A) CCL25, (B) CXCL10, (C) CXCL12, and (D) CXCL16. A *p*-value less than 0.05 was considered as significant.
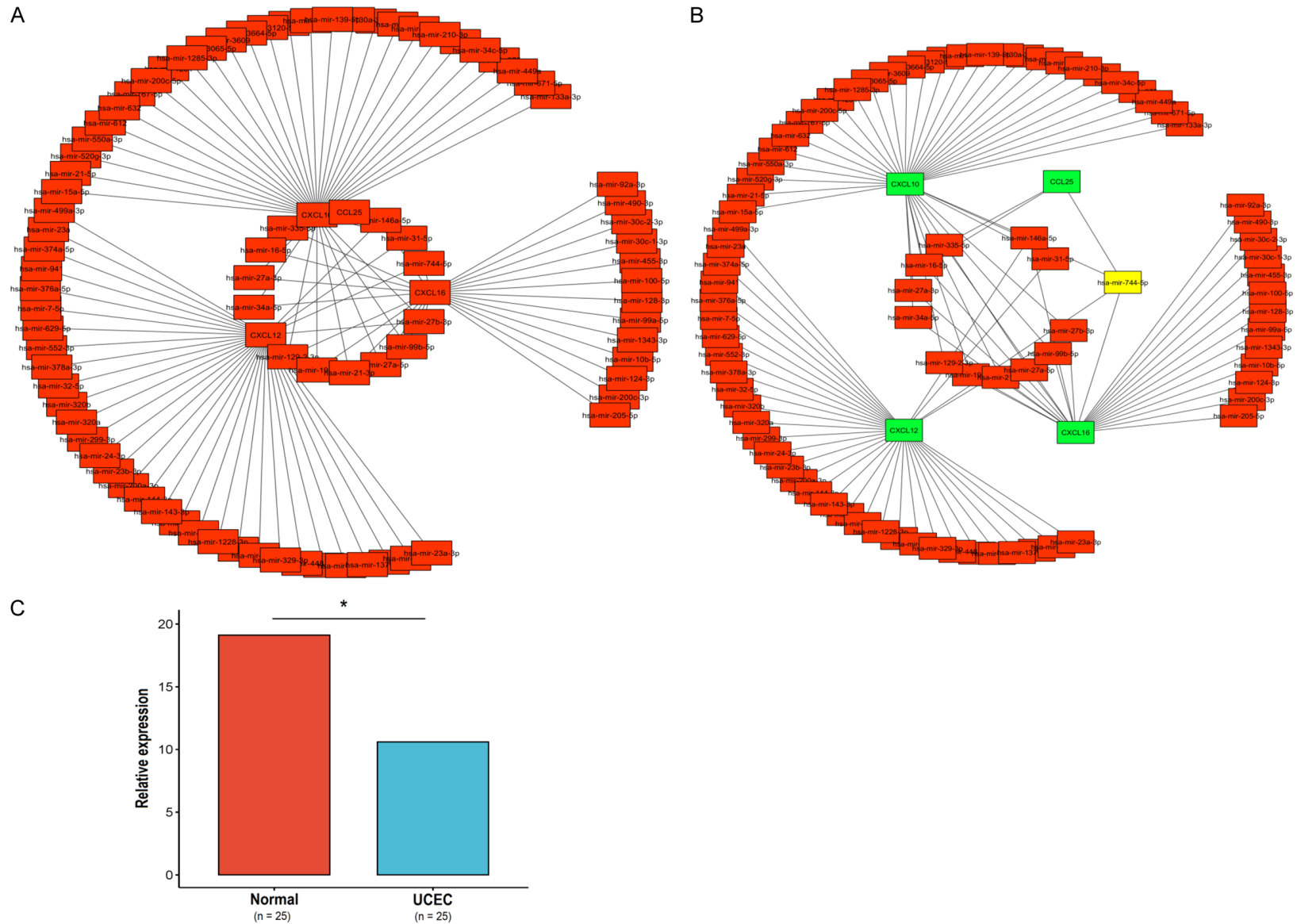
Figure 10. miRNA-mRNA co-regulatory network of CCL25, CXCL10, CXCL12, and CXCL16 hub genes. (A) A PPI of miRNAs targeting hub genes, (B) A PPI highlighting most important miRNA (hsa-mir-744-5p) targeting all hub genes, and (C) RT-qPCR based expression profiling of has-miR-27a-5p. A *p*-value less than 0.05 was considered as significant. miRNA, MicroRNA; mRNA, Messenger RNA; RT-qPCR, Reverse transcription-quantitative polymerase chain reaction.

Table 1. DrugBank-based hub genes-associated drugs

Sr. No	Hub gene	Drug name	Effect	Reference	Group
1	CCL25	Methotrexate	Decrease expression of CCL25 mRNA	A23201	Approved
		Acetylcysteine		A20451	
2	CXCL10	Acetaminophen	Decrease expression of CXCL10 mRNA	A20426	Approved
		Acteoside		A20456	
		Cyclosporine		A20661	
		Polydatin		A20456	
3	CXCL12	Belinostat	Increase expression of CXCL12 mRNA	A21037	Approved
		Decitabine		A21958	
		Mestranol		A21106	
4	CXCL16	Cyclosporine	Decrease expression of CXCL16 mRNA	A20661	Approved
		Estradiol		A21424	

mRNA, Messenger RNA; CCL25, CC motif chemokine ligand 25; CXCL10, C-X-C motif chemokine ligand 10; CXCL12, C-X-C motif chemokine ligand 12; CXCL16, C-X-C motif chemokine ligand 16.

To validate hsa-miR-744-5p as a common regulator of gene expression, we conducted RT-qPCR to analyze its expression in clinical UCEC sample group (n = 25) compared to the control group (n = 25). Our analysis demonstrated a significant decrease ($P < 0.05$) in the mRNA levels of hsa-miR-744-5p in UCEC group when compared to the control group (**Figure 10C**).

Drug prediction analysis of CCL25, CXCL10, CXCL12, and CXCL16

In the context of UCEC treatment, the initial approach typically involves medical intervention. Therefore, the identification of suitable candidate drugs becomes crucial. In our study, we utilized the DrugBank database to investigate potential drugs capable of reversing the gene expression of the identified hub genes for UCEC treatment. These drugs have been identified based on existing literature, computational analyses, and their known interactions with pathways associated with these hub genes. **Table 1** presents a range of drugs that have the potential to modulate the expression of CCL25, CXCL10, CXCL12, and CXCL16 during the treatment of UCEC. However, it's important to note that while these drugs demonstrate potential in silico and in vitro, their actual utility in clinical settings for UCEC treatment remains to be validated through rigorous experimental testing.

RT-qPCR validation analysis of CCL25, CXCL10, CXCL12, and CXCL16 in UCEC clinical tissue samples and cell lines

In order to validate our bioinformatics analysis, we performed an RT-qPCR experiment to quan-

tify the mRNA expression levels of the hub genes (CCL25, CXCL10, CXCL12, and CXCL16). This analysis was conducted using 25 paired UCEC tissue samples, as well as two endometrial adenocarcinoma cell lines (AN3CA, HTB-111 and HEC-1-A, HTB-112), and one normal endometrial cell line (HES). By directly measuring the gene expression in these samples and cell lines, we aimed to confirm the findings obtained through our bioinformatics analysis. **Figure 11A**, **11B** presents our findings, which demonstrate significant differences in the expression levels of the four hub genes (CCL25, CXCL10, CXCL12, and CXCL16) between the UCEC tissue samples and their paired controls, as well as in the UCEC cell lines and the normal control cell line. Interestingly, we observed an up-regulation of CCL25, CXCL10, and CXCL16, while CXCL12 exhibited down-regulation in both UCEC tissue samples and cell lines compared to the corresponding controls (**Figure 11A**, **11B**). Therefore, the experimental results of this study have successfully validated the bioinformatics-based findings, reinforcing the significance of our study. This validation is of utmost importance as it strengthens the reliability and credibility of our bioinformatics predictions. The consistency between the experimental and bioinformatics data provides strong evidence to support the identified hub genes and their regulatory networks.

Validation of the hub gene methylation status on cell lines

The validation of methylation levels in the hub gene was conducted through targeted bisulfite-
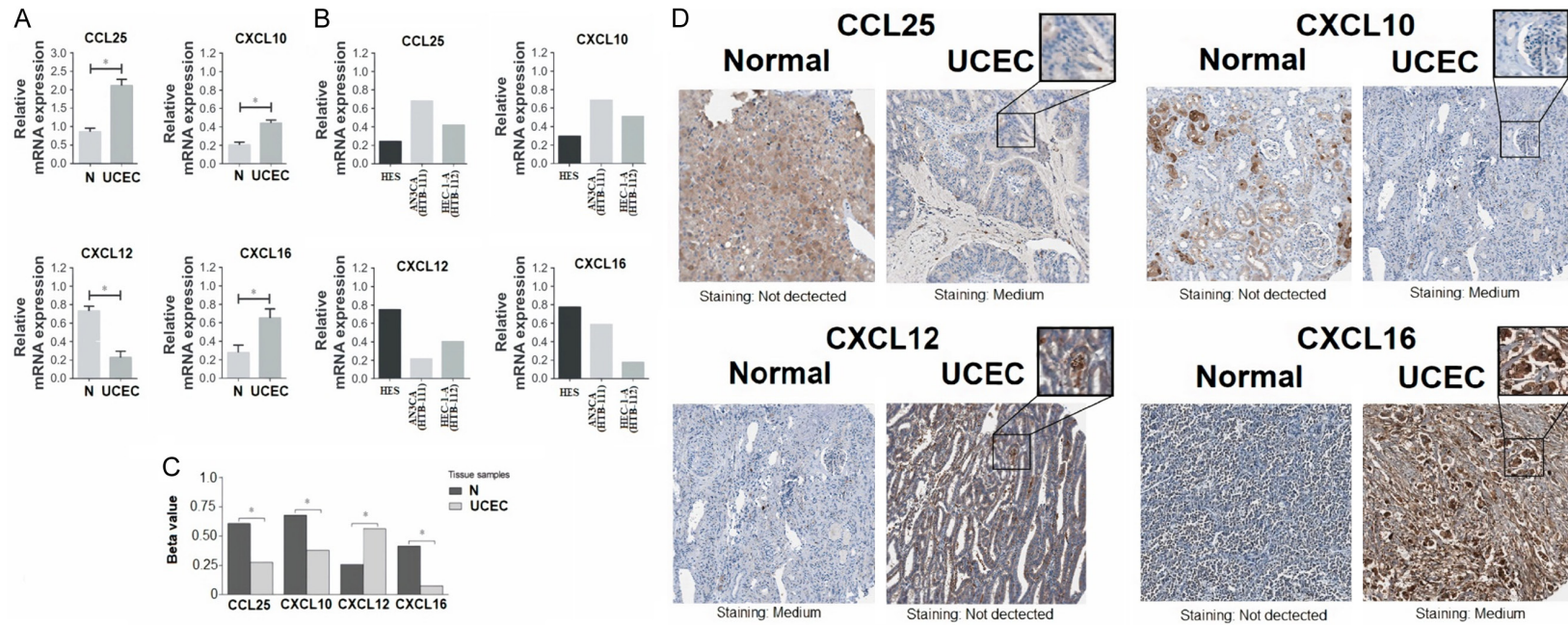
Figure 11. Validating CCL25, CXCL10, CXCL12, and CXCL16 expressions and promoter methylation levels using UCEC tissue samples and cell lines paired with controls via RT-qPCR and targeted bisulfite-seq analyses. (A) Relative expression profile of CCL25, CXCL10, CXCL12, and CXCL16 across UCEC tissue samples paired with controls via RT-qPCR, (B) Relative expression profile of CCL25, CXCL10, CXCL12, and CXCL16 using UCEC cell lines paired with control via RT-qPCR, (C) Beta values based promoter methylation based validation of CCL25, CXCL10, CXCL12, and CXCL16 across UCEC tissue samples paired with controls, and (D) IHC-based differential expression of CCL25, CXCL10, CXCL12, and CXCL16 in UCEC and normal tissues. A *p*-value less than 0.05 was considered as significant. UCEC, Uterine Corpus Endometrial Carcinoma; RT-qPCR, Reverse transcription-quantitative polymerase chain reaction.

seq analyses of two endometrial adenocarcinoma cell lines, namely AN3CA (HTB-111) and HEC-1-A (HTB-112), along with a normal endometrial cell line, HES. Beta values were utilized to validate the methylation levels in this analysis. The analysis results depicted in **Figure 11C** revealed notable differences in the beta values of the hub genes CCL25, CXCL10, CXCL12, and CXCL16 between the endometrial cell lines and the control cell line. Specifically, the beta values of CCL25, CXCL10, and CXCL16 were lower in the endometrial cell lines, while the beta value of CXCL12 was higher compared to the control cell line (**Figure 11C**).

CCL25, CXCL10, CXCL12, and CXCL16 gene expression in UCEC was verified by IHC in clinical samples

Upon analyzing the expression of CCL25, CXCL10, CXCL12, and CXCL16 using IHC, we observed distinct patterns in UCEC tissue samples compared to normal controls. Specifically, we found an up-regulation of CCL25, CXCL10, and CXCL16, indicated by medium staining intensity, in UCEC samples relative to normal counterpart. This suggests that these hub genes might be involved in promoting or facilitating UCEC development and progression. In contrast, CXCL12 expression was down-regulated and not detected in the UCEC samples relative to normal counterpart (**Figure 11D**). This finding implies that CXCL12 might play a distinct role in UCEC pathogenesis compared to the other hub genes.

Discussion

The molecular basis of UCEC remains largely unclear due to its complex etiology and genetic heterogeneity [46, 47]. Despite numerous research endeavors to unravel its pathogenesis and identify prognostic biomarkers, the prognosis for advanced UCEC remains unfavorable [48, 49]. Therefore, the objective of this study was to investigate key molecules associated with the development, progression, and prognosis of UCEC. In our present study, we employed a multi-layer approach to investigate the diagnostic and prognostic significance of the entire CC and CXC chemokine families in UCEC. Through our investigation, we discovered that CCL25, CXCL10, CXCL12, and CXCL16 stood out as the hub genes within the CC and CXC chemokine families. These particular

genes were designated as hubs due to their pivotal role and potential significance in UCEC. The identification of these hub genes underscores their importance in the development and advancement of the disease, shedding light on their potential involvement in the underlying mechanisms of UCEC. Moreover, across UCEC TCGA, samples, clinical samples, and cell lines, CCL25, CXCL10, and CXCL12 were remarkably increased, while CXCL12 was decreased compared to normal specimens. Additionally, our findings revealed that the hub genes identified in this study can serve as a reliable prognostic model for predicting the overall survival (OS) of UCEC patients.

CCL25 plays a critical role in cancer progression and metastasis [50]. This chemokine is primarily produced by the small intestine and functions by binding to its receptor CCR9, thereby regulating the migration and recruitment of immune cells to the gut mucosa [51]. However, dysregulation of the CCL25/CCR9 axis has been observed in various cancers, including colorectal, breast, and pancreatic cancer [52, 53]. Studies have demonstrated that overexpression of CCL25 promotes tumor cell proliferation, invasion, and angiogenesis, while inhibition or blockade of this chemokine leads to reduced tumor growth and metastasis [54]. For example, in breast cancer, the CCL25/CCR9 interaction has been shown to activate the Akt pathway, promoting cisplatin resistance in cancer cells [55]. In pancreatic cancer, the CCL25/CCR9 axis has been implicated in promoting cell proliferation, invasion, and metastasis [56]. Additionally, CCR9 expression has been identified as a prognostic marker for stage III colon cancer patients undergoing adjuvant chemotherapy [52], suggesting its potential as a therapeutic target.

CXCL10, plays a crucial role in cancer biology [57]. This chemokine is produced in response to interferon-gamma stimulation and is involved in modulating immune responses [57]. CXCL10 acts by binding to its receptor CXCR3, which is expressed on various immune cells and tumor cells [58]. Studies have shown that CXCL10 is dysregulated in several cancers, including breast, colorectal, lung, and pancreatic cancer [59, 60]. Elevated CXCL10 expression has been associated with tumor growth, angiogenesis, immune evasion, and metasta-

sis [61]. It promotes the recruitment of immune cells, such as T cells and natural killer cells, to the tumor microenvironment, influencing anti-tumor immune responses [62]. Moreover, CXCL10 has been suggested as a potential bio-marker for cancer prognosis and response to therapy [63].

CXCL12 plays a critical role in cancer progression and metastasis [64]. This chemokine is produced by stromal cells and acts through its receptor CXCR4, which is expressed on cancer cells [64]. Studies have shown that CXCL12 promotes cancer cell survival, migration, and invasion by stimulating signaling pathways involved in cell proliferation and cytoskeletal rearrangement [65]. It also enhances the recruitment of CXCR4-expressing cancer cells to specific organs, known as pre-metastatic niches, thereby facilitating the establishment of metastasis [66, 67]. Furthermore, CXCL12 can influence the tumor microenvironment by modulating immune responses, promoting immunosuppression, and affecting the recruitment and function of immune cells [66]. In colorectal cancer, dysregulation of CXCL12 contributes to tumor growth, angiogenesis, and poor prognosis [68]. In lung cancer, CXCL12 dysregulation is associated with increased invasion, migration, and angiogenesis [69]. CXCL12 dysregulation is also observed in pancreatic cancer, promoting tumor growth, invasion, and metastasis [70]. In prostate cancer, dysregulated CXCL12 expression is linked to an aggressive phenotype [71].

CXCL16, a transmembrane chemokine, plays a multifaceted role in human cancer [72]. This chemokine is expressed by various cell types, including tumor cells, endothelial cells, and immune cells [72]. CXCL16 functions through its receptor, CXCR6, and is involved in tumor growth, invasion, angiogenesis, and immune responses [73]. Studies have shown that CXCL16 expression is upregulated in several cancer types, such as breast, colorectal, lung, pancreatic, and prostate cancer. Elevated CXCL16 levels have been associated with aggressive tumor behavior, including increased invasiveness and metastasis [74, 75]. CXCL16 is also involved in tumor angiogenesis, promoting the formation of new blood vessels to support tumor growth [76]. Additionally, CXCL16 can modulate immune responses by attracting immune cells to the tumor microenvironment, potentially influencing antitumor immunity [76].

Regarding the mutational and methylation statuses of the CCL25, CXCL10, CXCL12, and CXCL16 genes, it was observed that these genes do not commonly undergo genetic mutations in UCEC. However, aberrant promoter methylation was found to be associated with elevated expression of CCL25, CXCL10, and CXCL16, and reduced expression of CXCL12. Several earlier studies have shown that CCL25, CXCL10, CXCL12, and CXCL16 genes are relatively stable and do not undergo significant genetic mutations [77, 78]. Consistent with previous studies, our findings align with the notion that the genes CCL25, CXCL10, CXCL12, and CXCL16 exhibit a lower frequency of genetic mutations in individuals diagnosed with cancer. These results corroborate the existing evidence suggesting a reduced incidence of mutations in these specific genes among cancer patients.

In this study, a noteworthy observation was made regarding the regulatory influence of hsa-mir-744-5p miRNA on the expression of CCL25, CXCL10, CXCL12, and CXCL16 hub genes in patients with UCEC. We found that these genes were simultaneously regulated by hsa-mir-744-5p, and their expression levels were significantly associated with the infiltration of immune cells such as CD8+ T cells, CD4+ T cells, and macrophages. Dysregulation of hsa-mir-744-5p has emerged as a significant molecular factor in cancer progression [79]. Studies have revealed the involvement of hsa-mir-744-5p in various cancer types, including breast, lung, colorectal, and ovarian cancer [80-83]. Dysregulated hsa-mir-744-5p promotes tumor growth by targeting key genes involved in cell cycle regulation, apoptosis, and metastasis. Understanding the intricate mechanisms of dysregulation and the downstream effects of hsa-mir-744-5p in cancer holds promise for the development of targeted therapies and diagnostic biomarkers. To our understanding, this research presents the initial evidence highlighting the potential cancer-promoting role of hsa-mir-744-5p miRNA in relation to CCL25, CXCL10, CXCL12, and CXCL16 hub genes in UCEC. This study represents the first of its kind to shed light on the probable involvement of hsa-mir-744-5p in driv-

ing cancer-related processes specifically associated with these hub genes. By uncovering this novel association, our findings contribute to the expanding knowledge of the intricate molecular mechanisms underlying UCEC development. Further investigations are warranted to fully elucidate the functional significance of hsa-mir-744-5p and its potential implications for targeted therapies in UCEC.

However, there were some limitations of the present study. Firstly, validation analysis thorugh qRT-PCR needs additional UCEC and paired normal tissues samples. Secondly, some more experiments, such as Western blot and iTRAQ, should be performed in future studies to confirm the protein levels of hub genes in UCEC.

Conclusion

This comprehensive study has led us to propose a model comprising four hub genes belonging to the CC and CXC gene families, which play a significant role in the initiation and progression of UCEC. These hub genes hold promising potential as reliable biomarkers for the diagnosis, prognosis, and treatment of UCEC patients. However, it is imperative to conduct further in-depth investigations to unravel the critical pathogenic roles of these genes in UCEC.

Disclosure of conflict of interest

None.

Address correspondence to: Faiqah Ramzan, Gomal Center of Bio-Chemistry and Biotechnology (GCBB), Gomal University, Dera Ismail Khan 29050, Pakistan. E-mail: faiqah.ramzan@gmail.com; Guiping Zhong, Health Management Center, The Second Affiliated Hospital of Hainan Medical University, Haikou 570311, Hainan, China. E-mail: ZGP060313@163.com

References

[1] Wang Y, Xu M and Yang Q. A six-microRNA signature predicts survival of patients with uterine corpus endometrial carcinoma. Curr Probl Cancer 2019; 43: 167-176.

[2] Pan Y, Jia LP, Liu Y, Han Y and Deng Q. Alteration of tumor associated neutrophils by PIK3CA expression in endometrial carcinoma from TCGA data. J Ovarian Res 2019; 12: 81.

[3] Usman M, Hameed Y, Ahmad M, Iqbal MJ, Maryam A, Mazhar A, Naz S, Tanveer R, Saeed H, Bint-E-Fatima, Ashraf A, Hadi A, Hameed Z, Tariq E and Aslam AS. SHMT2 is associated with tumor purity, CD8+ T immune cells infiltration, and a novel therapeutic target in four different human cancers. Curr Mol Med 2023; 23: 161-176.

[4] Tung HJ, Wu RC, Lin CY and Lai CH. Rare subtype of endometrial cancer: undifferentiated/dedifferentiated endometrial carcinoma, from genetic aspects to clinical practice. Int J Mol Sci 2022; 23: 3794.

[5] Wheelock CE, Goss VM, Balgoma D, Nicholas B, Brandsma J, Skipp PJ, Snowden S, Burg D, D'Amico A, Horvath I, Chaiboonchoe A, Ahmed H, Ballereau S, Rossios C, Chung KF, Montuschi P, Fowler SJ, Adcock IM, Postle AD, Dahlén SE, Rowe A, Sterk PJ, Auffray C and Djukanovic R; U-BIOPRED Study Group. Application of omics technologies to biomarker discovery in inflammatory lung diseases. Eur Respir J 2013; 42: 802-825.

[6] Mao J, Huang X, Okla MK, Abdel-Maksoud MA, Mubarak A, Hameed Z, Noreen R, Chaudhary A, Ghazanfar S, Liao Y, Hameed Y and Li C. Risk factors for TERT promoter mutations with papillary thyroid carcinoma patients: a meta-analysis and systematic review. Comput Math Methods Med 2022; 2022: 1721526.

[7] Ravegnini G, Gorini F, De Crescenzo E, De Leo A, De Biase D, Di Stanislao M, Hrelia P, Angelini S, De Iaco P and Perrone AM. Can miRNAs be useful biomarkers in improving prognostic stratification in endometrial cancer patients? An update review. Int J Cancer 2022; 150: 1077-1090.

[8] Song J, Im S, Lee SH and Jang HJ. Deep learning-based classification of uterine cervical and endometrial cancer subtypes from whole-slide histopathology images. Diagnostics (Basel) 2022; 12: 2623.

[9] García-Aranda M and Redondo M. Immunotherapy: a challenge of breast cancer treatment. Cancers (Basel) 2019; 11: 1822.

[10] Chow MT and Luster AD. Chemokines in cancer. Cancer Immunol Res 2014; 2: 1125-1131.

[11] Bikfalvi A and Billottet C. The CC and CXC chemokines: major regulators of tumor progression and the tumor microenvironment. Am J Physiol Cell Physiol 2020; 318: C542-C554.

[12] Moser B, Wolf M, Walz A and Loetscher P. Chemokines: multiple levels of leukocyte migration control. Trends Immunol 2004; 25: 75-84.

[13] Zlotnik A, Burkhardt AM and Homey B. Homeostatic chemokine receptors and organ-specific metastasis. Nat Rev Immunol 2011; 11: 597-606.

[14] Zlotnik A, Yoshie O and Nomiyama H. The chemokine and chemokine receptor superfamilies

and their molecular evolution. Genome Biol 2006; 7: 243.

[15] Chen K, Bao Z, Tang P, Gong W, Yoshimura T and Wang JM. Chemokines in homeostasis and diseases. Cell Mol Immunol 2018; 15: 324-334.

[16] Mollica Poeta V, Massara M, Capucetti A and Bonecchi R. Chemokines and chemokine receptors: new targets for cancer immunotherapy. Front Immunol 2019; 10: 379.

[17] Cabrero-de Las Heras S and Martínez-Balibrea E. CXC family of chemokines as prognostic or predictive biomarkers and possible drug targets in colorectal cancer. World J Gastroenterol 2018; 24: 4738-4749.

[18] Zhao QQ, Jiang C, Gao Q, Zhang YY, Wang G, Chen XP, Wu SB and Tang J. Gene expression and methylation profiles identified CXCL3 and CXCL8 as key genes for diagnosis and prognosis of colon adenocarcinoma. J Cell Physiol 2020; 235: 4902-4912.

[19] Cao Z, Fu B, Deng B, Zeng Y, Wan X and Qu L. Overexpression of Chemokine (C-X-C) ligand 1 (CXCL1) associated with tumor progression and poor prognosis in hepatocellular carcinoma. Cancer Cell Int 2014; 14: 86.

[20] Spaks A, Svirina D, Spaka I, Jaunalksne I, Breiva D, Tracums I and Krievins D. CXC chemokine ligand 4 (CXCL4) is predictor of tumour angiogenic activity and prognostic biomarker in non-small cell lung cancer (NSCLC) patients undergoing surgical treatment. Biomarkers 2016; 21: 474-478.

[21] Hwang TL, Lee LY, Wang CC, Liang Y, Huang SF and Wu CM. CCL7 and CCL21 overexpression in gastric cancer is associated with lymph node metastasis and poor prognosis. World J Gastroenterol 2012; 18: 1249-56.

[22] Frick VO, Rubie C, Kölsch K, Wagner M, Ghadjar P, Graeber S and Glanemann M. CCR6/CCL20 chemokine expression profile in distinct colorectal malignancies. Scand J Immunol 2013; 78: 298-305.

[23] von Mering C, Huynen M, Jaeggi D, Schmidt S, Bork P and Snel B. STRING: a database of predicted functional associations between proteins. Nucleic Acids Res 2003; 31: 258-261.

[24] Chin CH, Chen SH, Wu HH, Ho CW, Ko MT and Lin CY. cytoHubba: identifying hub objects and sub-networks from complex interactome. BMC Syst Biol 2014; 8 Suppl 4: S11.

[25] Pan X, Chen S, Chen X, Ren Q, Yue L, Niu S, Li Z, Zhu R, Chen X, Jia Z, Zhen R and Ban J. UTP14A, DKC1, DDX10, PinX1, and ESF1 modulate cardiac angiogenesis leading to obesity-induced cardiac injury. J Diabetes Res 2022; 2022: 2923291.

[26] Chandrashekar DS, Bashel B, Balasubramanya SAH, Creighton CJ, Ponce-Rodriguez I, Chakravarthi BVSK and Varambally S. UALCAN: a portal for facilitating tumor subgroup gene expression and survival analyses. Neoplasia 2017; 19: 649-658.

[27] Tang Z, Li C, Kang B, Gao G, Li C and Zhang Z. GEPIA: a web server for cancer and normal gene expression profiling and interactive analyses. Nucleic Acids Res 2017; 45: W98-W102.

[28] Tang G, Cho M and Wang X. OncoDB: an interactive online database for analysis of gene expression and viral infection in cancer. Nucleic Acids Res 2022; 50: D1334-D1339.

[29] Nagy Á and Győrffy B. muTarget: a platform linking gene expression changes and mutation status in solid tumors. Int J Cancer 2021; 148: 502-511.

[30] Dwivedi B, Mumme H, Satpathy S, Bhasin SS and Bhasin M. Survival genie, a web platform for survival analysis across pediatric and adult cancers. Sci Rep 2022; 12: 3069.

[31] Usman M, Hameed Y, Ahmad M, Jalil Ur Rehman, Ahmed H, Hussain MS, Asif R, Murtaza MG, Jawad MT and Iqbal MJ. Breast cancer risk and human papillomavirus infection: a Bradford Hill criteria based evaluation. Infect Disord Drug Targets 2022; 22: e200122200389.

[32] Koch A, De Meyer T, Jeschke J and Van Criekinge W. MEXPRESS: visualizing expression, DNA methylation and clinical TCGA data. BMC Genomics 2015; 16: 636.

[33] Gao J, Aksoy BA, Dogrusoz U, Dresdner G, Gross B, Sumer SO, Sun Y, Jacobsen A, Sinha R, Larsson E, Cerami E, Sander C and Schultz N. Integrative analysis of complex cancer genomics and clinical profiles using the cBioPortal. Sci Signal 2013; 6: pl1.

[34] Hameed Y, Usman M, Liang S and Ejaz S. Novel diagnostic and prognostic biomarkers of colorectal cancer: capable to overcome the heterogeneity-specific barrier and valid for global applications. PLos One 2021; 16: e0256020.

[35] Subramanian A, Tamayo P, Mootha VK, Mukherjee S, Ebert BL, Gillette MA, Paulovich A, Pomeroy SL, Golub TR, Lander ES and Mesirov JP. Gene set enrichment analysis: a knowledge-based approach for interpreting genome-wide expression profiles. Proc Natl Acad Sci U S A 2005; 102: 15545-15550.

[36] Li T, Fan J, Wang B, Traugh N, Chen Q, Liu JS, Li B and Liu XS. TIMER: a web server for comprehensive analysis of tumor-infiltrating immune cells. Cancer Res 2017; 77: e108-e110.

[37] Huang DP, Zeng YH, Yuan WQ, Huang XF, Chen SQ, Wang MY, Qiu YJ and Tong GD. Bioinformatics analyses of potential miRNA-mRNA regulatory axis in HBV-related hepatocellular carcinoma. Int J Med Sci 2021; 18: 335-346.

[38] Freshour SL, Kiwala S, Cotto KC, Coffman AC, McMichael JF, Song JJ, Griffith M, Griffith OL and Wagner AH. Integration of the drug-gene

interaction database (DGIdb 4.0) with open crowdsource efforts. Nucleic Acids Res 2021; 49: D1144-D1151.

[39] Livak KJ and Schmittgen TD. Analysis of relative gene expression data using real-time quantitative PCR and the 2(-delta delta C(T)) method. Methods 2001; 25: 402-408.

[40] Jafri HSMO, Mushtaq S and Baig S. Detection of Kras gene in colorectal cancer patients through liquid biopsy: a cost-effective method. J Coll Physicians Surg Pak 2021; 31: 1174-1178.

[41] Meurens F, Whale J, Brownlie R, Dybvig T, Thompson DR and Gerdts V. Expression of mucosal chemokines TECK/CCL25 and MEC/CCL28 during fetal development of the ovine mucosal immune system. Immunology 2007; 120: 544-555.

[42] Shi D, Li Y, Shi X, Yao M, Wu D, Zheng Y, Lin Q and Yang Y. Transcriptional expression of CXCL10 and STAT1 in lupus nephritis and the intervention effect of triptolide. Clin Rheumatol 2023; 42: 539-548.

[43] Li T, Li H, Wang Y, Harvard C, Tan JL, Au A, Xu Z, Jablons DM and You L. The expression of CXCR4, CXCL12 and CXCR7 in malignant pleural mesothelioma. J Pathol 2011; 223: 519-530.

[44] Lu Y, Wang J, Xu Y, Koch AE, Cai Z, Chen X, Galson DL, Taichman RS and Zhang J. CXCL16 functions as a novel chemotactic factor for prostate cancer cells in vitro. Mol Cancer Res 2008; 6: 546-554.

[45] Zhang W, Liao K and Liu D. MicroRNA-744-5p is downregulated in colorectal cancer and targets SEPT2 to suppress the malignant phenotype. Mol Med Rep 2021; 23: 54.

[46] Volpato CB, De Grandi A, Buffone E, Facheris M, Gebert U, Schifferle G, Schönhuber R, Hicks A and Pramstaller PP. 2q37 as a susceptibility locus for idiopathic basal ganglia calcification (IBGC) in a large South Tyrolean family. J Mol Neurosci 2009; 39: 346-353.

[47] Sial N, Rehman JU, Saeed S, Ahmad M, Hameed Y, Atif M, Rehman A, Asif R, Ahmed H, Hussain MS, Khan MR, Ambreen A and Ambreen A. Integrative analysis reveals methylenetetrahydrofolate dehydrogenase 1-like as an independent shared diagnostic and prognostic biomarker in five different human cancers. Biosci Rep 2022; 42: BSR20211783.

[48] Sial N, Saeed S, Ahmad M, Hameed Y, Rehman A, Abbas M, Asif R, Ahmed H, Hussain MS, Rehman JU, Atif M and Khan MR. Multi-omics analysis identified TMED2 as a shared potential biomarker in six subtypes of human cancer. Int J Gen Med 2021; 14: 7025-7042.

[49] Usman M, Okla MK, Asif HM, AbdElgayed G, Muccee F, Ghazanfar S, Ahmad M, Iqbal MJ, Sahar AM, Khaliq G, Shoaib R, Zaheer H and Hameed Y. A pan-cancer analysis of GINS complex subunit 4 to identify its potential role as a biomarker in multiple human cancers. Am J Cancer Res 2022; 12: 986-1008.

[50] Johnson-Holiday C, Singh R, Johnson E, Singh S, Stockard CR, Grizzle WE and Lillard JW Jr. CCL25 mediates migration, invasion and matrix metalloproteinase expression by breast cancer cells in a CCR9-dependent fashion. Int J Oncol 2011; 38: 1279-1285.

[51] Papadakis KA, Prehn J, Nelson V, Cheng L, Binder SW, Ponath PD, Andrew DP and Targan SR. The role of thymus-expressed chemokine and its receptor CCR9 on lymphocytes in the regional specialization of the mucosal immune system. J Immunol 2000; 165: 5069-5076.

[52] Bai M, Chen X and Ba Y. CXCL10/CXCR3 overexpression as a biomarker of poor prognosis in patients with stage II colorectal cancer. Mol Clin Oncol 2016; 4: 23-30.

[53] Korbecki J, Grochans S, Gutowska I, Barczak K and Baranowska-Bosiacka I. CC chemokines in a tumor: a review of pro-cancer and anti-cancer properties of receptors CCR5, CCR6, CCR7, CCR8, CCR9, and CCR10 ligands. Int J Mol Sci 2020; 21: 7619.

[54] Liu H, Yang Z, Lu W, Chen Z, Chen L, Han S, Wu X, Cai T and Cai Y. Chemokines and chemokine receptors: a new strategy for breast cancer therapy. Cancer Med 2020; 9: 3786-3799.

[55] Tu Z, Xiao R, Xiong J, Tembo KM, Deng X, Xiong M, Liu P, Wang M and Zhang Q. CCR9 in cancer: oncogenic role and therapeutic targeting. J Hematol Oncol 2016; 9: 10.

[56] Lee S, Heinrich EL, Li L, Lu J, Choi AH, Levy RA, Wagner JE, Yip ML, Vaidehi N and Kim J. CCR9-mediated signaling through β-catenin and identification of a novel CCR9 antagonist. Mol Oncol 2015; 9: 1599-1611.

[57] Piper KP, Horlock C, Curnow SJ, Arrazi J, Nicholls S, Mahendra P, Craddock C and Moss PA. CXCL10-CXCR3 interactions play an important role in the pathogenesis of acute graft-versus-host disease in the skin following allogeneic stem-cell transplantation. Blood 2007; 110: 3827-3832.

[58] Liu M, Guo S and Stiles JK. The emerging role of CXCL10 in cancer. Oncol Lett 2011; 2: 583-589.

[59] Westrich JA, Vermeer DW, Colbert PL, Spanos WC and Pyeon D. The multifarious roles of the chemokine CXCL14 in cancer progression and immune responses. Mol Carcinog 2020; 59: 794-806.

[60] Gowhari Shabgah A, Amir A, Gardanova ZR, Olegovna Zekiy A, Thangavelu L, Ebrahimi Nik M, Ahmadi M and Gholizadeh Navashenaq J. Interleukin-25: new perspective and state-of-the-art in cancer prognosis and treatment approaches. Cancer Med 2021; 10: 5191-5202.

[61] Tugues S, Honjo S, König C, Noguer O, Hedlund M, Botling J, Deschoemaeker S, Wenes M, Rolny C, Jahnen-Dechent W, Mazzone M and Claesson-Welsh L. Genetic deficiency in plasma protein HRG enhances tumor growth and metastasis by exacerbating immune escape and vessel abnormalizationtumor growth and spread in hrg deficiency. Cancer Res 2012; 72: 1953-1963.

[62] Anderson NM and Simon MC. The tumor microenvironment. Curr Biol 2020; 30: R921-R925.

[63] Gao X and Zhao S. miRNA-16-5p inhibits the apoptosis of high glucose-induced pancreatic β cells via targeting of CXCL10: potential biomarkers in type 1 diabetes mellitus. Endokrynol Pol 2020; 71: 404-410.

[64] Li B, Wang Z, Wu H, Xue M, Lin P, Wang S, Lin N, Huang X, Pan W, Liu M, Yan X, Qu H, Sun L, Li H, Wu Y, Teng W, Wang Z, Zhou X, Chen H, Poznansky MC and Ye Z. Epigenetic regulation of CXCL12 plays a critical role in mediating tumor progression and the immune response in osteosarcoma. Cancer Res 2018; 78: 3938-3953.

[65] Di J, Huang H, Qu D, Tang J, Cao W, Lu Z, Cheng Q, Yang J, Bai J, Zhang Y and Zheng J. Rap2B promotes proliferation, migration and invasion of human breast cancer through calcium-related ERK1/2 signaling pathway. Sci Rep 2015; 5: 12363.

[66] Liu Y and Cao X. Characteristics and significance of the pre-metastatic niche. Cancer Cell 2016; 30: 668-681.

[67] Hameed Y, Usman M and Ahmad M. Does mouse mammary tumor-like virus cause human breast cancer? Applying Bradford Hill criteria postulates. Bull Natl Res Cent 2020; 44: 183.

[68] Bocchi M, de Sousa Pereira N, de Oliveira KB and Amarante MK. Involvement of CXCL12/CXCR4 axis in colorectal cancer: a mini-review. Mol Biol Rep 2023; 50: 6233-6239.

[69] Tsai CN, Yu SC, Lee CW, Pang JS, Wu CH, Lin SE, Chung YH, Tsai CL, Hsieh SY and Yu MC. SOX4 activates CXCL12 in hepatocellular carcinoma cells to modulate endothelial cell migration and angiogenesis in vivo. Oncogene 2020; 39: 4695-4710.

[70] Shen B, Zheng MQ, Lu JW, Jiang Q, Wang TH and Huang XE. CXCL12-CXCR4 promotes proliferation and invasion of pancreatic cancer cells. Asian Pac J Cancer Prev 2013; 14: 5403-5408.

[71] Jung Y, Kim JK, Lee E, Cackowski FC, Decker AM, Krebsbach PH and Taichman RS. CXCL12γ induces human prostate and mammary gland development. Prostate 2020; 80: 1145-1156.

[72] Bao N, Fu B, Zhong X, Jia S, Ren Z, Wang H, Wang W, Shi H, Li J, Ge F, Chang Q, Gong Y, Liu W, Qiu F, Xu S and Li T. Role of the CXCR6/CXCL16 axis in autoimmune diseases. Int Immunopharmacol 2023; 121: 110530.

[73] Darash-Yahana M, Gillespie JW, Hewitt SM, Chen YY, Maeda S, Stein I, Singh SP, Bedolla RB, Peled A, Troyer DA, Pikarsky E, Karin M and Farber JM. The chemokine CXCL16 and its receptor, CXCR6, as markers and promoters of inflammation-associated cancers. PLoS One 2009; 4: e6695.

[74] Mir H, Kaur G, Kapur N, Bae S, Lillard JW Jr and Singh S. Higher CXCL16 exodomain is associated with aggressive ovarian cancer and promotes the disease by CXCR6 activation and MMP modulation. Sci Rep 2019; 9: 2527.

[75] Lee JT, Lee SD, Lee JZ, Chung MK and Ha HK. Expression analysis and clinical significance of CXCL16/CXCR6 in patients with bladder cancer. Oncol Lett 2013; 5: 229-235.

[76] Singh S, Sadanandam A and Singh RK. Chemokines in tumor angiogenesis and metastasis. Cancer Metastasis Rev 2007; 26: 453-467.

[77] Menzies FM, Oldham RS, Waddell C, Nelson SM and Nibbs RJB. A comprehensive profile of chemokine gene expression in the tissues of the female reproductive tract in mice. Immunol Invest 2020; 49: 264-286.

[78] Groblewska M, Litman-Zawadzka A and Mroczko B. The role of selected chemokines and their receptors in the development of gliomas. Int J Mol Sci 2020; 21: 3704.

[79] Huang W, Chen Q, Dai J, Zhang Y, Yi Y, Wei X and Wu Z. miR-744-5p suppresses tumor proliferation and metastasis by targeting transforming growth factor-beta 1 (TGF-β1) in hepatocellular carcinoma (HCC). J Gastrointest Oncol 2021; 12: 1811-1822.

[80] Liang H, Li L, Zhu S, Tan J, Yang B, Wang X, Wu G, Xie C, Li L, Liu Z, Li Y, Song H, Chen G and Lin L. MicroRNA-744-5p suppresses tumorigenesis and metastasis of osteosarcoma through the p38 mitogen-activated protein kinases pathway by targeting transforming growth factor-beta 1. Bioengineered 2022; 13: 12309-12325.

[81] Zhao LG, Wang J, Li J and Li QF. miR-744-5p inhibits cellular proliferation and invasion via targeting ARF1 in epithelial ovarian cancer. Kaohsiung J Med Sci 2020; 36: 799-807.

[82] Chen S, Shi F, Zhang W, Zhou Y and Huang J. miR-744-5p inhibits non-small cell lung cancer proliferation and invasion by directly targeting PAX2. Technol Cancer Res Treat 2019; 18: 1533033819876913.

[83] Kleemann M, Schneider H, Unger K, Sander P, Schneider EM, Fischer-Posovszky P, Handrick R and Otte K. MiR-744-5p inducing cell death by directly targeting HNRNPC and NFIX in ovarian cancer cells. Sci Rep 2018; 8: 9020.